Differential Diagnosis in Orthopaedic Oncology

Differential Diagnosis in Orthopaedic Oncology

SECOND EDITION

Adam Greenspan, M.D., F.A.C.R.
Professor Emeritus of Radiology and Orthopedic Surgery
Former Chief, Section of Musculoskeletal Imaging
Department of Radiology
University of California, Davis School of Medicine
Sacramento, California

Gernot Jundt, M.D.
Professor of Pathology
Head, Swiss Bone Tumor Reference Center
Institute of Pathology at the University of Basel
Basel, Switzerland

Wolfgang Remagen, M.D.
Professor Emeritus of Pathology
Senior Consultant
Swiss Bone Tumor Reference Center
Institute of Pathology at the University of Basel
Basel, Switzerland

Lippincott Williams & Wilkins
a Wolters Kluwer business
Philadelphia • Baltimore • New York • London
Buenos Aires • Hong Kong • Sydney • Tokyo

Acquisitions Editor: Lisa McAllister
Managing Editor: Kerry Barrett
Project Manager: Fran Gunning
Senior Manufacturing Manager: Benjamin Rivera
Marketing Manager: Angela Panetta
Creative Director: Stephen Druding
Production Services: Nesbitt Graphics, Inc.
Printer: R.R. Donnelley, Shenzhen, China

530 Walnut Street
Philadelphia, PA 19106 USA
LWW.com

First edition, © 1998 Lippincott-Raven Publishers

Printed in China

Library of Congress Cataloging-in-Publication Data

Greenspan, Adam.
Differential diagnosis in orthopaedic oncology / Adam Greenspan, Gernot Jundt, Wolfgang Remagen.—2nd ed.
p. ; cm.
Rev. ed. of: Differential diagnosis of tumors and tumor-like lesions of bones and joints/ Adam Greenspan and Wolfgang Remagen. 1997.
Includes bibliographical references and index.
ISBN 978-0-7817-7930-2 (alk. paper)
1. Bones—Tumors—Diagnosis. 2. Joints—Tumors—Diagnosis. 3. Diagnosis, Differential. I. Jundt, Gernot. II. Remagen, Wolfgang. III. Greenspan, Adam. Differential diagnosis of tumors and tumor-like lesions of bones and joints. IV. Title.
[DNLM: 1. Bone Neoplasms—diagnosis. 2. Diagnosis, Differential. 3. Joint Diseases—diagnosis. 4. Soft Tissue Neoplasms—diagnosis. WE 258 G815d 2007]
RC280.B6G74 2007
616.99′471075–dc22

2006020800

To purchase additional copies of this book, call our customer service department at (800)638-3030 or fax orders to (301) 223-2320. International customers should call (301) 223-2300.

Visit Lippincott Williams & Wilkins on the Internet: at LWW.com. Lippincott Williams & Wilkins customer service representatives are available from 8:30 am to 6 pm, EST.

10 9 8 7 6 5 4 3 2 1

To my wife Barbara, my children Michael, Samantha, and Luddy, and my grandchildren Anna and Sydney, with love; and to the memory of my mother Eugenia, and my father Bernard, a brilliant physician, who taught me my ABC's of the medical profession.

–A.G.

To Inge for her constant support and encouragement while I took time off from her to work on this book.

–G.J.

To my wife Karin for her patience, understanding, and encouragement.

–W.R.

Contents

Preface

The first edition of this text, titled *Differential Diagnosis of Tumors and Tumor-like Lesions of Bones and Joints,* was published in 1998. The past eight years have brought significant changes to the imaging of musculoskeletal lesions, as well as changes in the pathologic classification of many of the tumors. In particular, further technological advances in the field of radiology, mainly technical improvements in orthopaedic imaging of bone and soft tissue tumors using positron emission tomography (PET), computed tomography (thin-section CT and 3-D CT studies), and magnetic resonance imaging (MRI), as well as wide use of enzyme histochemistry, immunohistochemistry, and genetics (flow cytometry, cytogenetics, and molecular cytogenetics) in pathology, prompted the need for a new edition of this book. The title has been changed to *Differential Diagnosis in Orthopaedic Oncology,* and although the main emphasis is on lesions of the bones and joints, some of the soft tissue tumors have also been included (the scope of this text precluded discussion of all the soft tissue tumors). A new co-author has been added; he is Gernot Jundt, M.D., Professor of Pathology at the Bone Tumor Reference Center of the Institute of Pathology, University Hospital in Basel, Switzerland. Dr. Jundt is a panelist of the Working Group of the World Health Organization (WHO), the body that, in 2002, revised the old classification and proposed a new classification of several tumors of soft tissue and bone. This addition guarantees inclusion of the most up-to-date information on histopathologic classification and differential diagnosis of musculoskeletal lesions.

As in the first edition, the thrust of this text is facilitation of the complex differential diagnosis of bone and joint tumors and tumor-like lesions that confronts the radiologist, pathologist, and orthopaedic oncologist. Again, the emphasis is on radiologic and histopathologic approaches to the same lesion, because the differential diagnosis of a given tumor considered by the radiologist may vary from that considered by the pathologist. The text provides an overview of the diverse radiologic and histopathologic appearances of benign and malignant musculoskeletal lesions, including typical and atypical features. Each chapter presents information concerning clinical presentation of the lesion, imaging techniques and radiologic features, histopathology, and radiologic and pathologic differential diagnosis. Pathology sections stress the use of immunohistochemistry and genetics as they are applied to differential diagnosis. As in the previous edition, the chapters are richly illustrated with radiographs, CT and MR images, photomicrographs in color, and schematic drawings. Important diagnostic features are provided in concise tables, and a summary of differential diagnoses (both radiologic and pathologic) is included at the end of each section in the form of a schematic drawing that also depicts the less likely possibilities not discussed in the text.

There are many changes, additions, and improvements in this new edition. The book has received a new design, and the Table of Contents is now more detailed. The captions for the illustrations have been improved, with the diagnosis placed at the beginning of the legend in boldface type. Technically suboptimal figures have been either deleted or substituted with better-quality images (particularly in the pathology sections). Outdated text and references have been deleted and replaced with current ones. The text has been revised to include additional MRIs, CTs, and 3-D CT images. Several new sections have been added to almost every chapter. For example, in Chapter 1 the latest information on PET has been included. Also revised are the pathology sections, with addition of basic techniques and methods of decalcification, special stains, enzyme histochemistry, immunohistochemistry, and genetics in bone tumors. Chapter 2 has been completely rewritten, with addition of new material, particularly on bone island, osteosarcoma associated with syndromes, and description of new developments in cytogenetics and molecular cytogenetics of bone-forming tumors, both of which are on the cutting edge of research into these lesions. Moreover, the new classification of osteosarcomas has been added in the form of a diagram. Chapter 3 includes new text on myxoid chondrosarcoma, and significant changes have been made to the section discussing extraskeletal chondrosarcomas. In Chapter 4 more information on Jaffe-Campanacci and Mazabraud syndromes has been provided, along with new material on focal fibrocartilaginous dysplasia of long bones, pachydysostosis of the fibula, and liposclerosing myxofibrous tumor of bone. The reader will also find the recently revised concepts on fibrosarcoma and malignant fibrous histiocytoma. Because of the latest viewpoints on the so-called small, blue round cell tumors of bone and their classification, this section in Chapter 5 had to be substantially rewritten to include differential diagnoses based on genetic alterations. Similarly, because of new approaches to benign

and malignant vascular lesions, particularly the recent redefinition of biological classification of vascular anomalies and a recent attempt by WHO to clarify the existing nomenclature for malignant vascular tumors, Chapter 6 required substantial revision. Minor changes have been also made in Chapters 7 to 9; however, all chapters have received up-to-date references.

The histopathologic material, with a few exceptions, was obtained from the Swiss Bone Tumor Reference Center at the Institute of Pathology, University of Basel, Switzerland.

This text has been written primarily for the audience of radiologists, pathologists, and orthopaedic oncologists, although other physicians interested in orthopaedic oncology may also find it useful.

Adam Greenspan
Gernot Jundt
Wolfgang Remagen

Acknowledgments

We would like to acknowledge the guidance and help received in the preparation of this text from our friends at Lippincott Williams & Wilkins in Philadelphia, Pennsylvania. In particular, Lisa McAllister, Executive Editor, was instrumental in launching the second edition of this book, and Kerry Barrett, Senior Managing Editor, demonstrated effective coordination skills during all phases of preparation of this volume. Special thanks go to Stephen Druding, Design Coordinator, to Joseph DePinho, who designed the cover, and to Bill Donnelly at WT Design, who redesigned the interior of the book.

We also would like to thank several individuals from the Department of Radiology, UC Davis Medical Center in Sacramento, California. A special note of acknowledgment goes to Deborah Hoang for timely preparation of the manuscript, to Angela Michelier for her invaluable secretarial assistance, and to Julie Ostoich, senior photographer, and Aaron Peterson, for help in creating some digital illustrations.

Thomas Schürch and Jan Schwegler from University Hospital in Basel, Switzerland, are acknowledged for electronic reproduction of the radiographs and gross pathologic sections, and Petra Huber for constant help with finding cases, histopathologic slides and radiographs, and preparation of references. We are grateful to Sharon Rule for her meticulous editing of some of the sections of this book. Finally, we would like to express our gratitude to Joanne (Bonnie) Boehme, a Project Manager from Nesbitt Graphics, for supervision and help during the final composition of this text.

As with the previous edition, this project could not have been successfully completed without the prudent and dutiful efforts of the many individuals acknowledged here.

CHAPTER 1

Radiologic and Pathologic Approach to Bone Tumors

The ideal therapeutic goals for managing patients with primary or metastatic lesions can be incorporated into a triad of important factors: (a) do not overtreat a benign bone tumor; (b) do not undertreat a malignant bone tumor; and (c) do not take an incorrect biopsy approach to the lesion, because this may suggest a need for radical rather than more conservative surgery (117,133,155). Achieving these goals depends on close cooperation among the radiologist, the pathologist, and the tumor surgeon (7,75,83).

Several factors make precise diagnosis of osseous tumors difficult. Although radiographic features have a high correlation with malignancy, benignity, and sometimes even an exact histologic diagnosis, radiographic determination of these characteristics is based on statistical probabilities. Moreover, errors in the radiologic interpretation may occur. These can usually be ascribed to failure to recognize a specific pathologic finding or to misinterpretation of normal structures as pathologic. Regardless of how persuasive a radiologist's clinical assessment of the biologic potential of a lesion may be to a pathologist colleague, any lesion, no matter how radiologically typical it appears, may represent an entirely different entity on histologic examination (68). A confident radiologic diagnosis may not outweigh the microscopic appearance of the lesion.

Both the radiologist and the pathologist play important roles by providing the diagnosis and/or differential diagnosis of a bone tumor, thus aiding the clinician in the complex process of patient management. Before a final diagnosis or differential diagnosis is made, clinical

information, radiologic imaging, and pathologic material should be carefully studied and correlated. The radiologist has the significant advantage of being able to view the three-dimensional extent of a bone tumor, whereas the pathologist can view only a small biopsy specimen of the lesion selected by the surgeon (133), which may not reflect the histology of the entire lesion. Obviously, viewing the entire resected specimen enhances the final pathologic evaluation. Many years ago, Ewing commented that "the gross anatomy (as revealed in radiographs) is often a safer guide to a correct clinical conception of the disease than the variable and uncertain nature of a small piece of tissue" (48). It is important to emphasize that the differential diagnosis contemplated by the radiologist may be identical to or different from that contemplated by the pathologist. For example, a radiologist who is evaluating a lesion that looks like an aneurysmal bone cyst must include in the differential diagnosis the possibility of telangiectatic osteosarcoma. Likewise, the pathologist who is looking at the histologic sections of the same lesion must also consider the possibility of telangiectatic osteosarcoma because both lesions have several histopathologic similarities. On the other hand, in the radiologic evaluation of a purely lytic lesion at the articular end of a long bone that looks like a giant cell tumor, plasmacytoma might enter into the differential diagnosis, whereas for a pathologist examining the same lesion (which in fact *is* a giant cell tumor), the differential diagnosis will obviously include other lesions that may contain giant cells. However, the pathologist would not consider plasmacytoma as one of the differential possibilities because of the completely different histologic pattern of this tumor.

For teaching purposes, the diagnostic approach to bone tumors is discussed separately from the radiologic and the pathologic point of view.

Radiology

In general, the imaging of musculoskeletal neoplasms can be considered from three standpoints: detection, diagnosis and differential diagnosis, and evaluation (staging) (Fig. 1-1). Detection of a bone tumor does not always require the expertise of a radiologist. The clinical history and the physical examination are often sufficient to raise the suspicion of a tumor, although radiography is the most common means of revealing one. Skeletal scintigraphy can also pinpoint lesions, but its findings are nonspecific.

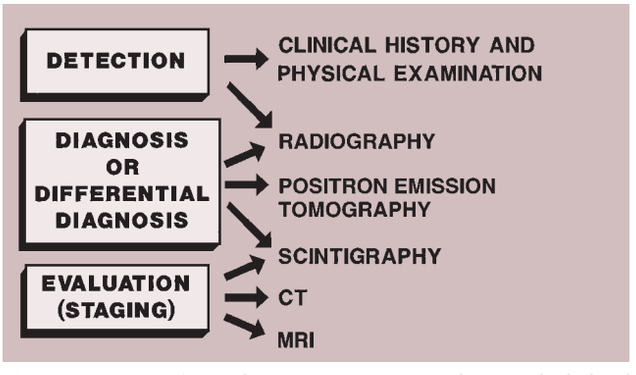

Figure 1-1 Imaging of tumors. Imaging of musculoskeletal neoplasms can be considered from three aspects: detection, diagnosis (or differential diagnosis), and evaluation.

Despite the dramatic advances in imaging technology that have occurred in recent decades, especially the introduction of cross-sectional imaging modalities such as computed tomography (CT) and magnetic resonance imaging (MRI), radiography remains the single most important modality for establishing a diagnosis (69) and serves as the basis for differential diagnosis (37,115,136). It yields the most useful information about the location and morphology of a lesion, particularly concerning the type of bone destruction, calcifications, ossifications, and periosteal reaction. Conventional tomography, although presently rarely implemented, can be a useful diagnostic tool, particularly on those occasions when questions arise regarding cortical destruction, periosteal reaction, or mineralization of the tumor matrix. It can also detect occult pathologic fracture (1). Scintigraphy is only occasionally helpful in making a specific diagnosis but can be valuable in distinguishing, for example, multiple myeloma from similar-appearing metastases (121) or for distinguishing a benign or malignant sclerotic tumor from a bone island (70).

The imaging advances of the past decade have been most profoundly felt in the evaluation (staging) of bone tumors (46,102,144,145). The multiplanar capabilities and unsurpassed soft tissue contrast offered by CT (24,114) and MRI (10,11,103) have rendered these modalities indispensable in tumor staging (15,33,57,64, 148). They have enabled radiologists to determine tumor size, location, and configuration more accurately than ever before and have facilitated demonstration of intra- and extramedullary extension of tumors and the relationship of tumors to individual muscles, muscle compartments, fascial planes, and neurovascular bundles, as well as to neighboring joints and organs (12,13, 189). MRI, in fact, affords more accurate anatomic staging than any other imaging method (19,20,32). Nevertheless, it is rarely helpful in differentiating benign from malignant tumors, despite attempts to identify signal intensity patterns, the appearance of tumor margins, the presence of edema, and neurovascular bundle involvement as markers for this essential determination (76,93).

Other techniques also play roles in evaluation of bone tumors. These include scintigraphic techniques using technetium (Tc-99), gallium citrate (Ga-67), and indium (In-111)–labeled white blood cells, as well as single photon emission computed tomography (SPECT), among others (12,13,47,55,92,121,189). Because these imaging methods use radiopharmaceutical labeling, they can provide information about the pathophysiologic function of bone and surrounding soft tissues, as well as the size and location of a lesion (120).

Most recently the application of positron emission tomography (PET) for diagnosis of musculoskeletal neoplasms gained a worldwide acceptance (2,21,104,182). PET differs from other single-photon radionuclide scans in its ability to correct for tissue attenuation signal loss

and its relatively uniform spatial resolution (52). This technique contributes unique information regarding metabolism of musculoskeletal lesions (51) based on observations of high glycolysis rates in malignant tissues (186). In particular, whole-body ^{18}F-labeled 2-fluoro-2-deoxyglucose (^{18}FDG)-PET scanning is a valuable adjunct in identifying primary, recurrent, and metastatic cartilage malignancies (52).

Arteriography is used mainly to map out bone lesion and to assess the extent of disease. It is also used to demonstrate the vascular supply of a tumor and to localize vessels suitable for preoperative intraarterial chemotherapy as well as to demonstrate the area suitable for open biopsy, because the most vascular parts of a tumor contain the most aggressive components. Occasionally, arteriography can be used to demonstrate abnormal tumor vessels, corroborating findings revealed by radiography. In selected cases, this technique may help to differentiate osteoid osteoma from bone abscess.

Ultrasonography only rarely contributes information useful in differential diagnosis of malignant and benign musculoskeletal tumors (18).

Radiography

Conventional radiographs continue to provide a wealth of information whose implications can be helpful in the precise diagnosis of a bone tumor (69,96,106,140, 192,210). However, radiography does not provide a diagnosis in every case (86). Some types of tumor can be diagnosed with certainty by their radiographic appearance alone, other types can be diagnosed only with various degrees of probability, and still others may have an appearance compatible with that of more than one type of tumor and therefore allow only a differential diagnosis to be made (134,163). The information yielded by radiography includes (Fig. 1-2):

- Topography of the lesion (location in the skeleton and in the individual bone)
- Borders of the lesion (the so-called zone of transition)
- Type of bone destruction
- Type of periosteal response to the lesion (periosteal reaction)
- Type of matrix of the lesion (composition of the tumor tissue)
- Nature and extent of soft tissue involvement

Patient age and determination of whether a lesion is solitary or multiple are the starting approaches in the diagnosis of bone tumors (Fig. 1-3). The age of the patient is the single most important item of clinical data that can be used in conjunction with the radiographic findings to establish a diagnosis (99). Certain tumors occur almost exclusively in a specific age group (Fig. 1-4). For example, aneurysmal bone cyst, chondromyxoid fibroma, and chondroblastoma rarely occur in individuals older than 20 years. Conversely, giant cell tumor of bone almost invariably arises after growth plate closure, and metastatic lesions, myeloma, and conventional chondrosarcoma are rarely encountered in patients younger than 40 years

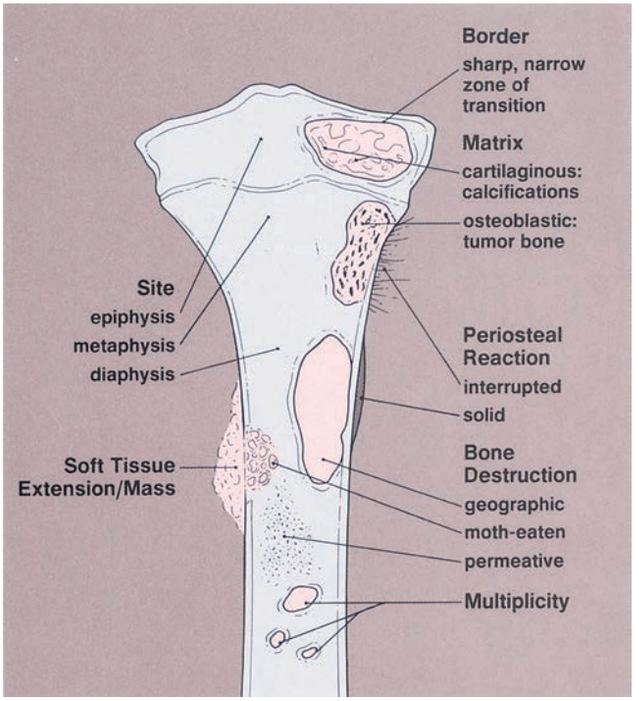

Figure 1-2 Radiographic features of tumors and tumor-like lesions of bone.

(105,108). Some bone tumors associated with specific age groups may have different radiographic presentations and appear in atypical locations, when they arise outside of their usual age population. Simple bone cysts, for example, are found almost exclusively in the long bones (proximal humerus, proximal femur) before skeletal maturity. After skeletal maturity they may arise in the pelvis, scapula, or calcaneus, among other sites, and may exhibit unconventional radiographic features with progressing age (141).

Determining the number of lesions also has important implications. Benign lesions tend to involve multi-

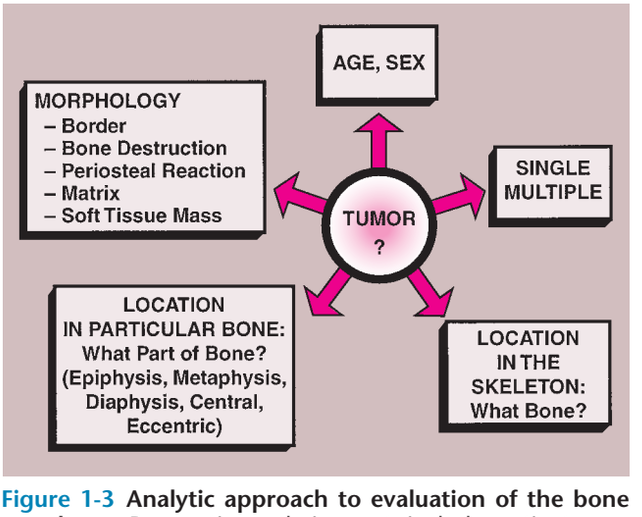

Figure 1-3 Analytic approach to evaluation of the bone neoplasm. Pragmatic analysis must include patient age, multiplicity of a lesion, location in the skeleton and in the particular bone, and radiographic morphology.

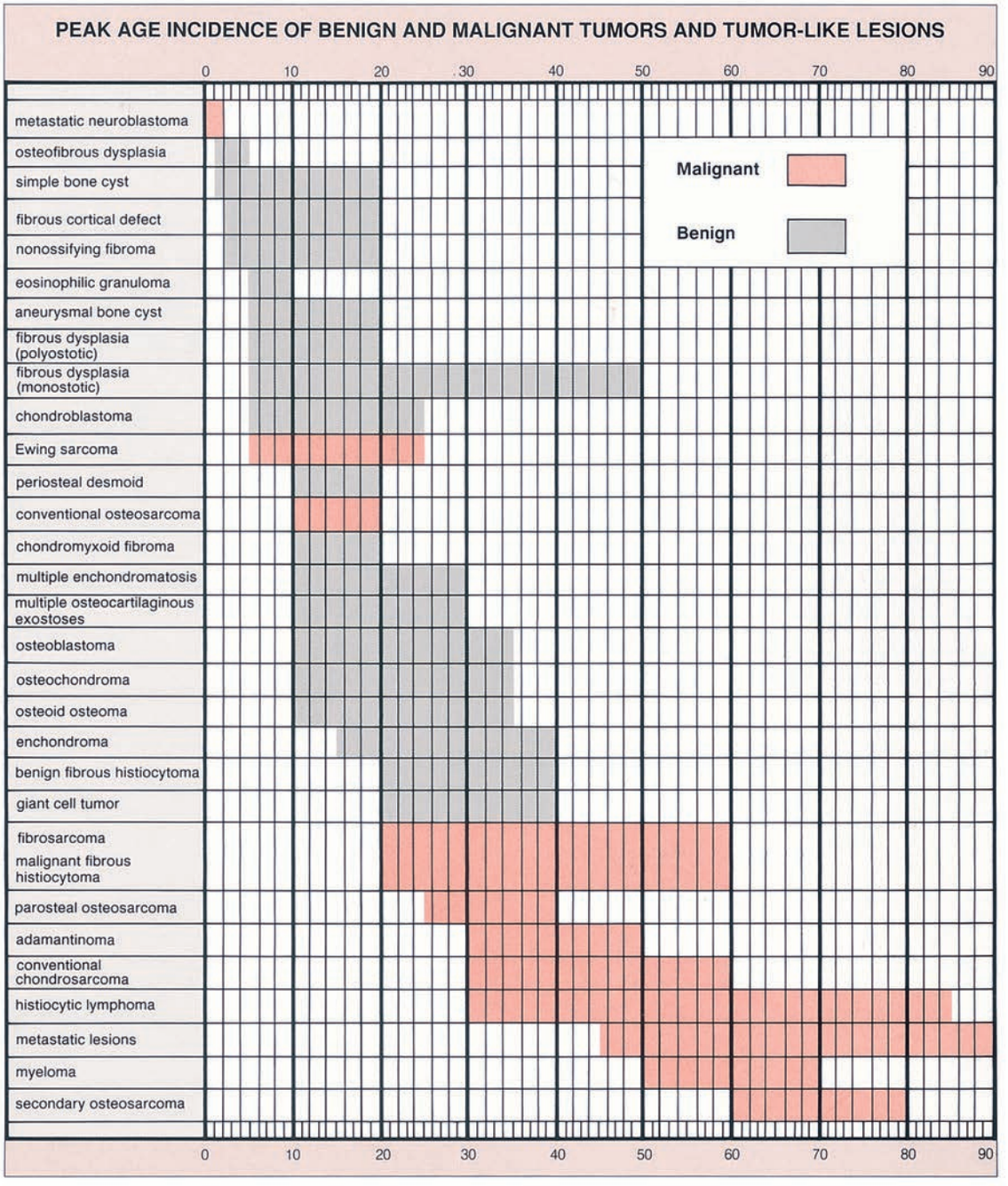

Figure 1-4 **Peak age incidence of some benign and malignant tumors and tumor-like lesions.**

ple sites, as in polyostotic fibrous dysplasia, enchondromatosis, multiple osteocartilaginous exostoses, Langerhans cell histiocytosis (eosinophilic granuloma), hemangiomatosis, and fibromatosis. In contrast, primary malignancies, such as osteosarcoma, Ewing sarcoma, fibrosarcoma, and malignant fibrous histiocytoma, rarely present as multifocal disease. Multiple malignant lesions usually indicate metastatic disease, multiple myeloma, or lymphoma.

Site of the Lesion

Some tumors have a predilection for specific bones or specific sites in bone (Table 1-1 and Fig. 1-5). This location is determined by the laws of field behavior and developmental anatomy of the affected bone, a concept first popularized by Johnson (84,133). Parosteal osteosarcoma, for example, arises with very rare exceptions in the posterior aspect of the distal femur, a feature so characteristic that it alone can suggest the diagnosis (Fig. 1-6). The same can be said of chondroblastoma, which has a strong preference for the epiphysis of long bones before skeletal maturity (Fig. 1-7). Adamantinoma and osteofibrous dysplasia have a specific predilection for the tibia (Fig. 1-8; see also Figs. 4-49, 4-50, and 7-64). A lesion's location can also exclude certain entities from the differential diagnosis.

Table 1-1 **Predilection of Tumors for Specific Sites in the Skeleton**

	A. Skeletal Predilection of Benign Osseous Neoplasms and Tumor-like Lesions	B. Skeletal Predilection of Malignant Osseous Neoplasms
Axial skeleton	*Skull and facial bones:* Osteoma, osteoblastoma, Langerhans cell histiocytosis, fibrous dysplasia, solitary hemangioma, osteoporosis circumscripta (lytic phase of Paget disease) *Jaw:* Giant cell reparative granuloma, myxoma, ossifying fibroma, desmoplastic fibroma *Spine:* Aneurysmal bone cyst, osteoblastoma, Langerhans cell histiocytosis, hemangioma	*Skull and facial bones:* Mesenchymal chondrosarcoma, chordoma, multiple myeloma, metastatic neuroblastoma, metastatic carcinoma *Mandible:* Osteosarcoma, myeloma *Spine:* Chordoma, myeloma, metastases
Appendicular skeleton	*Long tubular bones:* Osteoid osteoma, simple bone cyst, aneurysmal bone cyst, osteochondroma, enchondroma, periosteal chondroma, chondroblastoma, chondromyxoid fibroma, nonossifying fibroma, giant cell tumor, osteofibrous dysplasia, desmoplastic fibroma, intraosseous ganglion *Hands and feet:* Giant cell reparative granuloma, florid reactive periostitis, enchondroma, glomus tumor, epidermoid cyst, subungual exostosis, bizarre parosteal osteochondromatous lesion	*Long tubular bones:* Osteosarcoma (all variants), adamantinoma, malignant fibrous histiocytoma, fibrosarcoma, primary lymphoma, chondrosarcoma, angiosarcoma *Hands and feet:* None
Specific predilections	Simple bone cyst—proximal humerus, proximal femur Osteofibrous dysplasia—tibia, fibula (anterior cortex) Focal fibrocartilaginous dysplasia of long bones—proximal metaphysis of tibia Osteoid osteoma—femur, tibia Chondromyxoid fibroma—tibia, metaphyses Chondroblastoma—epiphyses Giant cell tumor—articular ends of femur, tibia, radius Liposclerosing myxofibrous tumor—intertrochanteric region of femur	Adamantinoma—tibia, fibula Parosteal osteosarcoma—distal femur (posterior cortex) Periosteal osteosarcoma—tibia Chondrosarcoma (conventional)—femur, humerus, pelvic bones Clear cell chondrosarcoma—proximal femur and humerus Chordoma—sacrum, clivus, C2 Multiple myeloma—pelvis, spine, skull

Modified from Fechner RE, Mills SE. *Tumors of the bones and joints,* 3rd ed., Vol. 8. Washington, DC: Armed Forces Institute of Pathology, 1993:1–16.

Giant cell tumor, for example, should not be seriously considered if the lesion does not affect the articular end of a bone because very few of these tumors are found anywhere else.

Equally important in the evaluation of a lesion's site is its location in relation to the central axis of the bone (Fig. 1-9). This is particularly true when the lesion is located in a long tubular bone, such as humerus, radius, femur, or tibia (71). For example, simple bone cyst, enchondroma, or a focus of fibrous dysplasia always appears centrally located (see Figs. 3-6B, 3-8, 3-9, 4-25, 7-17, and 7-18). In contrast, eccentric location is characteristically observed in aneurysmal bone cyst, chondromyxoid fibroma, and nonossifying fibroma (see Figs. 3-74, 3-75, 4-2B, 4-3, 4-4, 7-31, and 7-33).

Borders of the Lesion

The borders or margins of a lesion are crucial factors in determining the growth rate of a lesion and hence whether it is benign or malignant (113). Three types of lesion margins are encountered: (a) a margin with sharp demarcation by sclerosis between the peripheral aspect of the tumor and the adjacent host bone (IA margin), (b) a margin with sharp demarcation without sclerosis around the periphery of the lesion (IB margin), and (c) a margin with an ill-defined region (either the entire circumference or only a portion of it) at the interface between lesion and host bone (IC margin) (Fig. 1-10). Slow-growing lesions are marked by sharply outlined, sclerotic borders, and this narrow zone of transition usually indicates that a tumor is benign (133). Benign lesions such as nonossifying fibroma, simple bone cyst, and chondromyxoid fibroma almost invariably exhibit sclerosis at their borders (Fig. 1-11A). Indistinct borders (a wide zone of transition), on the other hand, are typical of malignant or aggressive lesions (Fig. 1-11B). Primary malignancies such as fibrosarcoma, malignant fibrous histiocytoma, lymphoma, multiple myeloma (or solitary plasmacytoma), and metastases from primary tumors of the kidney, thyroid, and gastrointestinal tract usually lack a sclerotic border, as does the giant cell tumor of bone. Radio- or chemotherapy of malignant bone tumors can alter their appearance, causing them to exhibit sclerosis and a narrow zone of transition (54).

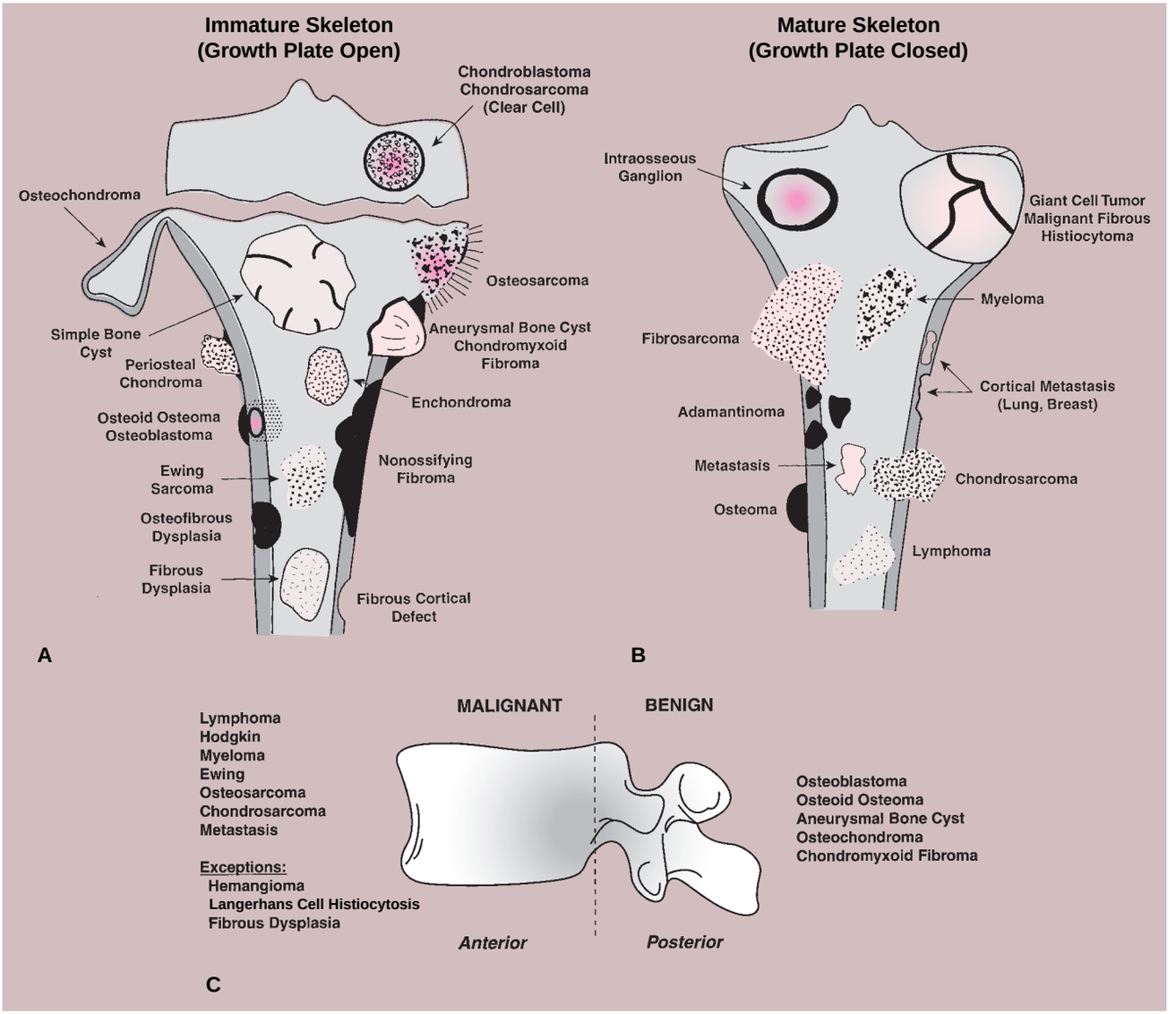

Figure 1-5 **Site of the lesion. A:** Distribution of various lesions in a long tubular bone in a growing skeleton (growth plate is open). **B:** Distribution of various lesions in a long tubular bone after skeletal maturity (growth plate is closed). **C:** Distribution of various lesions in a vertebra. Malignant lesions are seen predominantly in its anterior part (body), whereas benign lesions predominate in its posterior elements.

The more well defined the margin (e.g., IA, IB), the slower the biologic activity, and therefore the more likely that the lesion is benign. Conversely, the less well defined the margin (IC), the greater the biologic activity, and therefore the more likely that the lesion is malignant (79,107).

Type of Bone Destruction

Destruction of bone represents not only a direct effect of tumor cells but also reflects a complex mechanism in which normal osteoclasts of the host bone respond to pressure generated by the enlarging mass and by active hyperemia associated with the tumor (134). Cortical bone is destroyed less rapidly than trabecular bone. However, loss of cortical bone appears earlier on radiography because its density is highly homogeneous compared with that of trabecular bone. In the latter, greater amounts of bone must be destroyed (about 70% loss of mineral content) before the loss becomes radiographically evident (134). Like the borders of a lesion, the type of bone destruction caused by a tumor indicates its growth rate. Bone destruction can be described as geographic (type I), moth-eaten (type II), and permeative (type III) (105,107) (Fig. 1-12). Although none of these features are pathognomonic for any specific neoplasm, the type of destruction may suggest a benign or a malignant process. Geographic bone destruction is characterized by a uniformly destroyed area usually within sharply defined borders. It typifies slow-growing, benign lesions, such as simple bone cyst, enchondroma, chondromyxoid fibroma, or giant cell tumor. On the other hand, moth-eaten (i.e., characterized by multiple, small,

Text continues on page 11

Figure 1-6 Site of the lesion. Parosteal osteosarcoma has a predilection for the posterior aspect of the distal femur.

Figure 1-8 Site of the lesion. The tibia is a common site for adamantinoma.

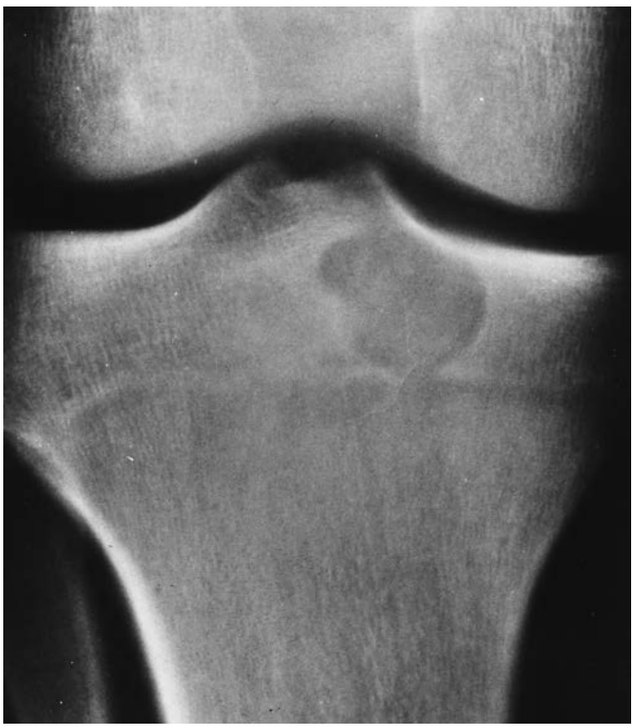

Figure 1-7 Site of the lesion. Chondroblastoma has a predilection for the epiphysis of a long bone.

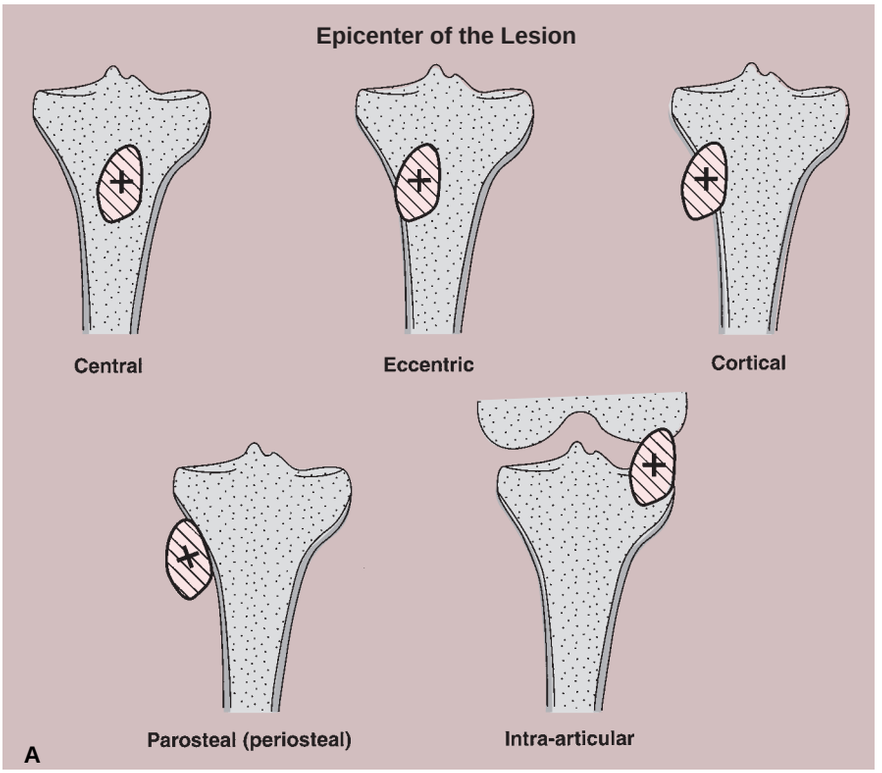

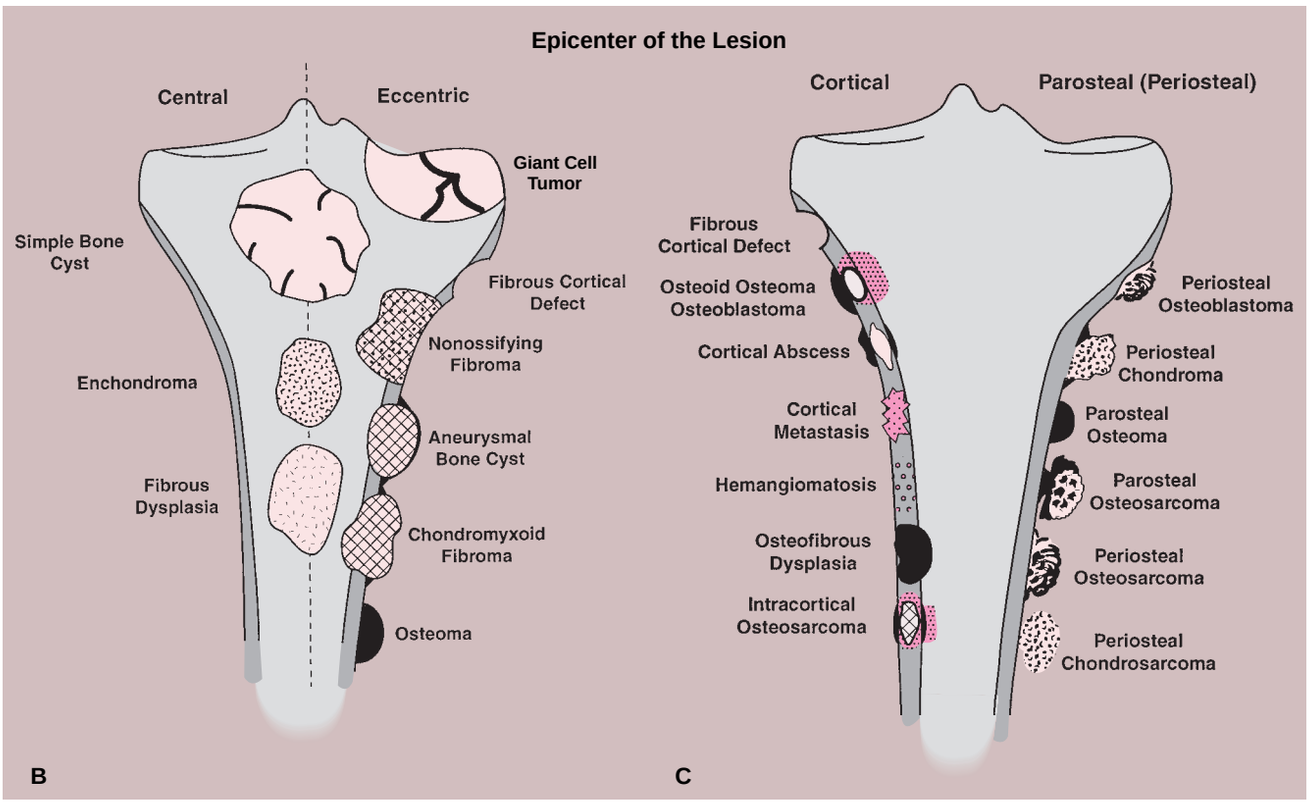

Figure 1-9 **Site of the lesion. A:** Location of the epicenter of the lesion usually determines the site of its origin, whether medullary, cortical, periosteal, soft tissue, or in the joint. **B:** Eccentric versus central location of the similar-appearing lesions is helpful in differential diagnosis. **C:** Cortical and parosteal (periosteal) lesions.

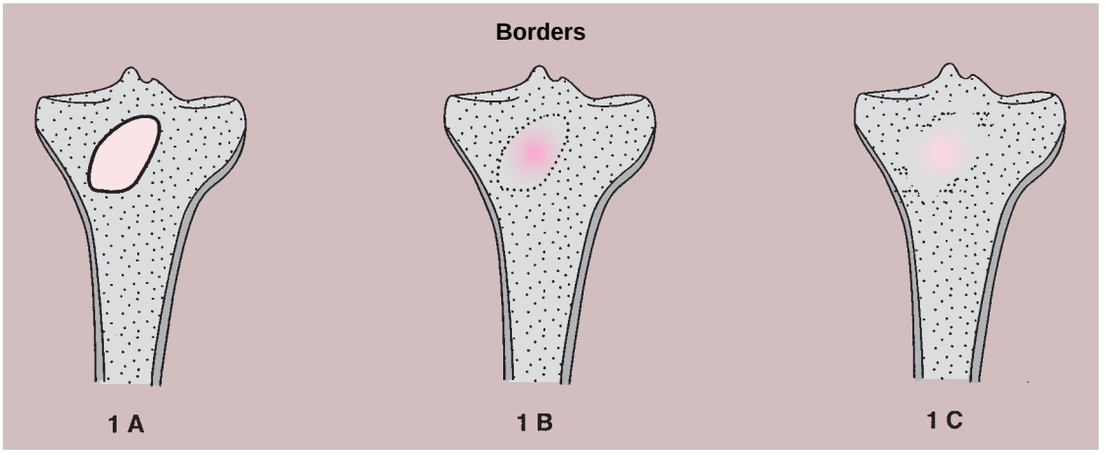

Figure 1-10 Borders of the lesion. Borders of the lesion determine its growth rate. *1A,* sharp sclerotic; *1B,* sharp lytic; *1C,* ill-defined. (Modified from Madewell JE, Ragsdale BD, Sweet DE. Radiologic and pathologic analysis of solitary bone lesions. Part I. Internal margins. *Radiol Clin North Am* 1981;19:715–748.)

Figure 1-11 Borders of the lesion. A: Sclerotic border or narrow zone of transition from normal to abnormal bone typifies a benign lesion, as in this example of nonossifying fibroma in the distal femur. **B:** A wide zone of transition typifies an aggressive or malignant lesion, in this case a plasmacytoma involving the pubic bone and supraacetabular portion of the right ilium. (Reprinted with permission from Greenspan A. *Orthopedic imaging,* 4th ed. Philadelphia: Lippincott Williams & Wilkins, 2004.)

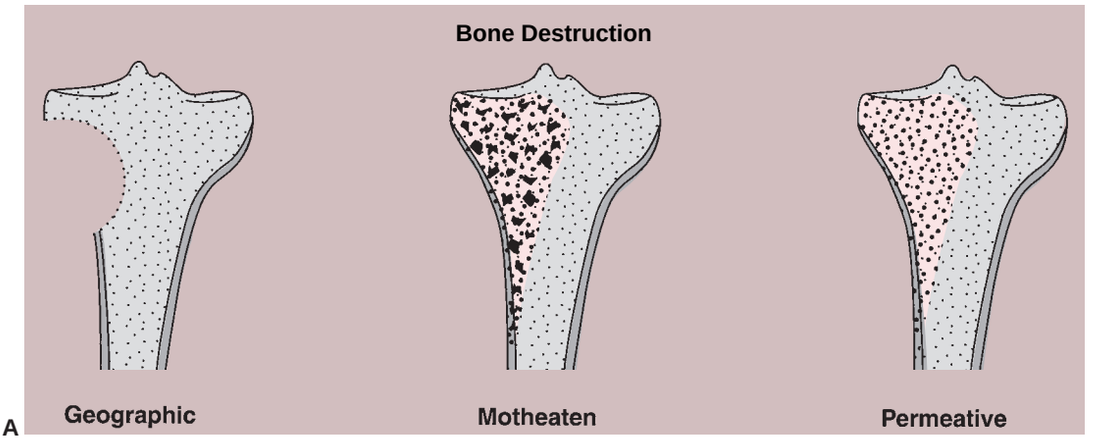

A

B

C

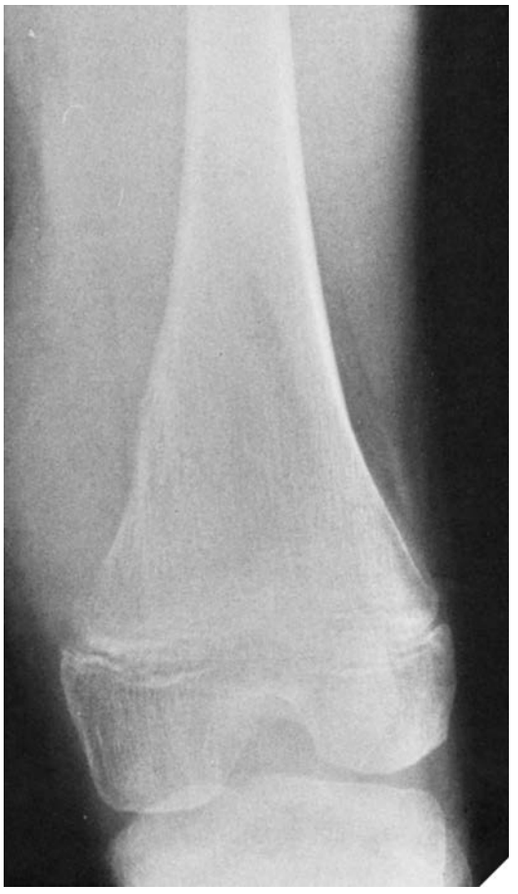

D

Figure 1-12 Patterns of bone destruction. A: Three types of bone destruction determine the lesion's growth rate. (Modified from Madewell JE, Ragsdale BD, Sweet DE. Radiologic and pathologic analysis of solitary bone lesions. Part I. Internal margins. *Radiol Clin North Am* 1981; 19:715–748.) **B:** The geographic type of bone destruction is characterized by a uniformly affected area within sharply defined borders, in this case a giant cell tumor. **C:** The moth-eaten bone destruction is characteristic of rapidly growing infiltrating lesions, in this case myeloma. **D:** The permeative type of bone destruction is characteristic of round cell tumors, in this case Ewing sarcoma. Note the almost imperceptible destruction of the metaphysis of the femur by a tumor that has infiltrated the medullary cavity and cortex and extended into the surrounding soft tissues, forming a large mass.

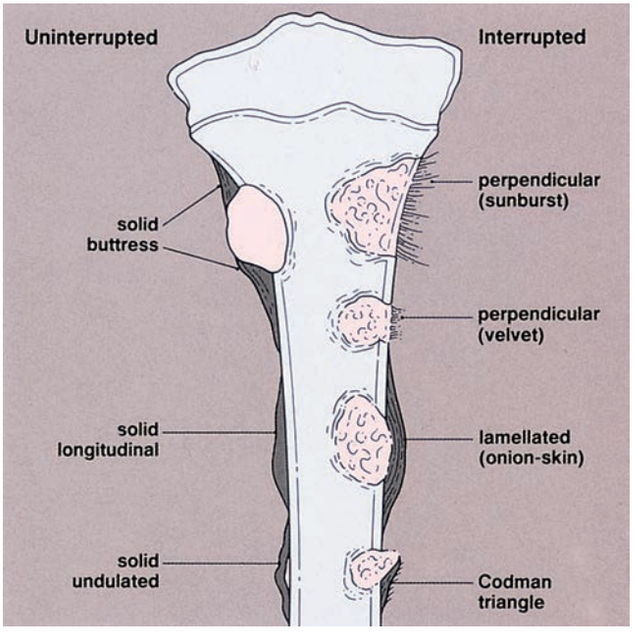

Figure 1-13 Types of periosteal reaction. An uninterrupted periosteal reaction usually indicates a benign process, whereas an interrupted reaction indicates a malignant or aggressive nonmalignant process.

often clustered lytic areas) and permeative (i.e., characterized by ill-defined, very small oval radiolucencies or lucent streaks) types of bone destruction mark rapidly growing, infiltrating tumors, such as myeloma, lymphoma, fibrosarcoma, or Ewing sarcoma. However, some nonneoplastic lesions may demonstrate this aggressive pattern. For example, osteomyelitis can exhibit both type II (moth-eaten) and type III (permeative) patterns of destruction (133). Similarly, hyperparathyroidism can cause a permeative pattern (113). The distinction between a moth-eaten and a permeative pattern of destruction may be subtle; often the two patterns coexist in the same lesion.

Periosteal Response

Like the pattern of bone destruction, the pattern of periosteal reaction is an indicator of the biologic activity of a lesion (209). Bone neoplasms elicit periosteal reactions that can be categorized as uninterrupted (continuous) or interrupted (discontinuous) (160) (Fig. 1-13 and Table 1-2). Any widening and irregularity of bone contour may represent periosteal activity. The solid periosteal reaction represents a single solid layer or multiple closely apposed and fused layers of new bone attached to the outer surface of the cortex (160) (Fig. 1-14). The resulting pattern is often referred to as cortical thickening (49). Although no single periosteal response is unique for a given lesion, an uninterrupted periosteal reaction indicates a long-standing (slow-growing), usually indolent, benign process. There are several types of solid periosteal reaction: a solid buttress, such as is frequently seen accompanying aneurysmal bone cyst and chondromyxoid fibroma; a solid smooth or elliptical layer, such as is seen in osteoid osteoma and osteoblastoma; an undulating type, most frequently seen in long-standing varicosities, pulmonary osteoarthropathy, chronic lymphedema, periostitis, and, rarely, with neoplasms (160); and a single lamellar reaction, such as accompanies osteomyelitis,

Table 1-2 **Examples of Nonneoplastic and Neoplastic Processes Categorized by Type of Periosteal Reaction**

Uninterrupted Periosteal Reaction	
Benign tumors and tumor-like lesions	*Nonneoplastic conditions*
Osteoid osteoma	Osteomyelitis
Osteoblastoma	Langerhans cell histiocytosis
Aneurysmal bone cyst	Healing fracture
Chondromyxoid fibroma	Juxtacortical myositis ossificans
Periosteal chondroma	Hypertrophic pulmonary osteoarthropathy
Chondroblastoma	Hemophilia (subperiosteal bleeding)
	Varicose veins and peripheral vascular insufficiency
Malignant tumors	Caffey disease
Chondrosarcoma (rare)	Thyroid acropachy
	Treated scurvy
	Pachydermoperiostosis
	Gaucher disease
Interrupted Periosteal Reaction	
Malignant tumors	*Nonneoplastic conditions*
Osteosarcoma	Osteomyelitis (occasionally)
Ewing sarcoma	Langerhans cell histiocytosis (occasionally)
Chondrosarcoma	Subperiosteal hemorrhage (occasionally)
Lymphoma (rare)	
Fibrosarcoma (rare)	
MFH (rare)	
Metastatic carcinoma	

Figure 1-14 Solid type of periosteal reaction. A: An uninterrupted solid periosteal reaction is characteristic of benign lesions, in this case a cortical osteoid osteoma. **B:** An uninterrupted periosteal reaction typifies changes of hypertrophic pulmonary osteoarthropathy as seen here in the distal radius and ulna and bones of the hand in a patient with carcinoma of the lung.

Langerhans cell histiocytosis, and stress fracture. An interrupted periosteal response, on the other hand, is commonly seen in malignant primary tumors and less commonly in some metastatic lesions and highly aggressive nonmalignant processes. In these tumors, the periosteal reaction may appear in a sunburst ("hair-on-end") (Fig. 1-15A) or onion-skin (lamellated) pattern (Fig. 1-15B,C). When the tumor breaks through the cortex and destroys the newly formed lamellated bone, the remnants of the latter on both ends of the breakthrough area may remain as a triangular structure known as a Codman triangle (Fig. 1-15D,E).

Type of Matrix

The matrix represents the intercellular material produced by mesenchymal cells and includes osteoid, bone, chondroid, myxoid, and collagen material (196). Assessment of the type of matrix allows differentiation of some similar-appearing lesions and, in particular, the tumor matrix provides a useful means of differentiating osteoblastic from chondroblastic processes. Although it should be kept in mind that tumor bone is often radiographically indistinguishable from reparative new bone deposited secondary to bone destruction by a reactive sclerosis or callus formation, the presence of irregular, not fully mineralized bone matrix within or adjacent to an area of bone destruction strongly suggests osteosarcoma (Fig. 1-16). Similarly, cottony or cloudlike densities within the medullary cavity and in the adjacent soft tissues are likely to represent tumor bone and hence osteosarcoma.

Calcifications in the tumor matrix, on the other hand, point to a chondroblastic process. These calcifications typically appear punctate (stippled), irregularly shaped (flocculent), or curvilinear (annular or comma-shaped, rings and arcs). In benign or well-differentiated malignant tumors they may reflect the process of endochondral ossification (196) (Fig. 1-17A). Differential diagnosis of stippled, flocculent, or ring-and-arc calcifications includes enchondroma (Fig. 1-17B), chondroblastoma, and chondrosarcoma (Fig. 1-17C). Sometimes it is difficult to distinguish osseous matrix from cartilaginous matrix. The former usually appears radiographically more organized and structural (trabecular), whereas the latter is more amorphous, with frequently distinguished characteristic calcifications (described previously).

A completely radiolucent lesion may be either fibrous or cartilaginous in origin, although hollow structures produced by tumor-like lesions, such as simple bone cysts or intraosseous ganglion, can also present as radiolucent areas (Table 1-3).

Text continues on page 17

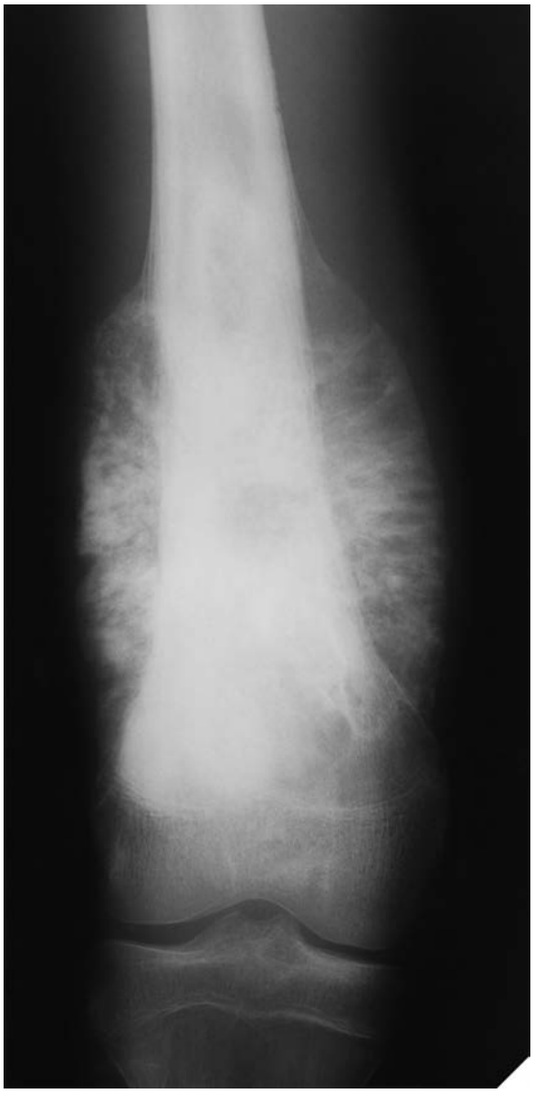

A

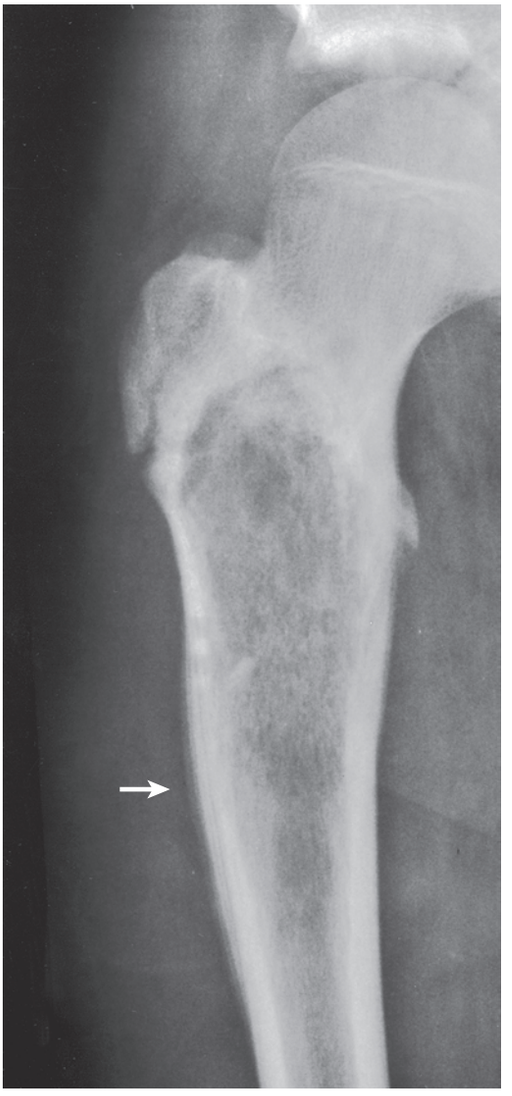

B

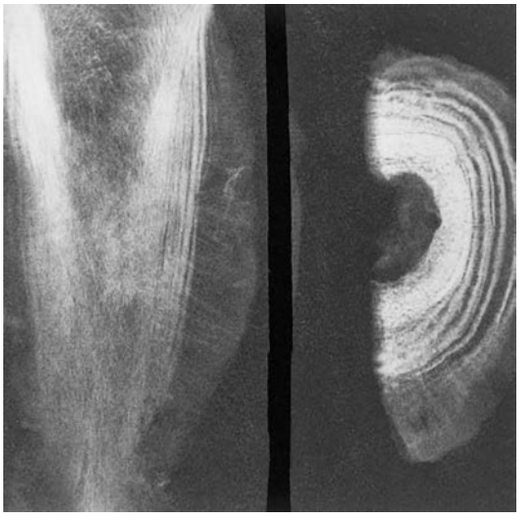

C

Figure 1-15 Interrupted type of periosteal reaction. A: Highly aggressive and malignant lesions may present radiographically with a sunburst pattern of periosteal reaction, as seen in this case of osteosarcoma. **B:** Another pattern of interrupted periosteal reaction is the lamellated or onion-skin type (*arrow*) as seen here in Ewing sarcoma involving the proximal femur. **C:** Radiographs of the slab sections (coronal at left and transverse at right) of the resected specimen from Ewing sarcoma demonstrate the lamellated type in more detail *(continued).*

D

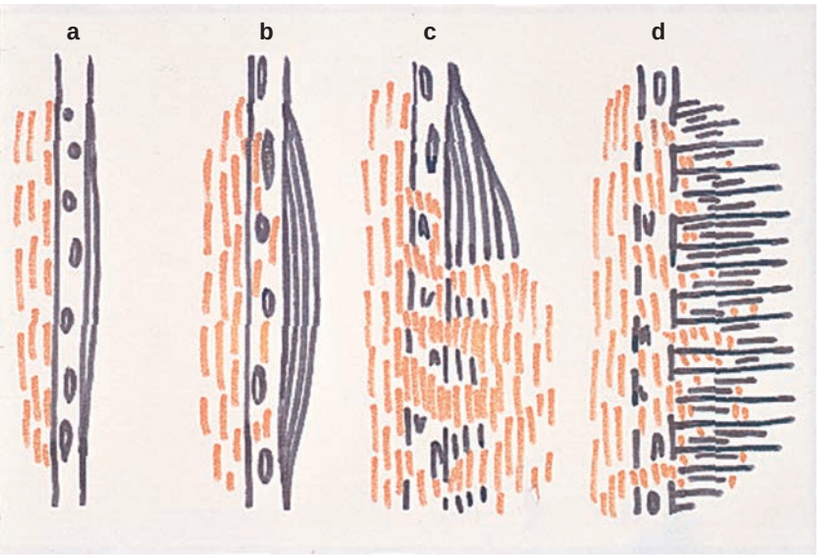

E

Figure 1-15 ***Continued*** **D:** Codman triangle (*arrow*) also reflects an aggressive, usually malignant type of periosteal response. **E:** Schematic representation of periosteal reactive bone formation. (a) Tumor (*red dashes*) growing against the endosteal border of the cortex blocks vascular supply and provokes reactive hyperemia of periosteum with secondary formation of a single layer of bone. (b) With progressive destruction of cortical bone, additional layers of periosteal bone form lamellated ("onion-peel") appearance. (c) After the rapidly growing tumor has destroyed cortex and newly formed periosteal bone, remnants of the latter at the tumor border form a Codman triangle. (d) Slowly growing tumor leaves time to form perpendicular reactive periosteal bone (spiculae, sunburst appearance).

Table 1-3 **Tumors and Pseudotumors That May Present as Radiolucent Lesions**

A. Solid	B. Cystic
Osteoblastic (osteoid osteoma, osteoblastoma, osteosarcoma, low-grade central osteosarcoma, telangiectatic osteosarcoma)	Simple bone cyst
Cartilaginous (enchondroma, chondroblastoma, chondromyxoid fibroma, chondrosarcoma)	Aneurystmal bone cyst
Fibrous and histiocytic (fibrous cortical defect, nonossifying fibroma, fibrous dysplasia, osteofibrous dysplasia, desmoplastic fibroma, fibrosarcoma, malignant fibrous histiocytoma)	Various bone cysts (synovial, degenerative)
Intraosseous lipoma	Hydatid cyst
Lymphoma	Brown tumor of hyperparathyroidism
Myeloma (plasmacytoma)	Vascular lesions
Ewing sarcoma	Hemophilic pseudotumor
Metastatic (from lung, breast, gastrointestinal tract, kidney, thyroid)	Intraosseous ganglion
Giant cell tumor	Bone abscess
Giant cell reparative granuloma	Cystic tuberculosis
Langerhans cell histiocytosis	
Paget disease (osteolytic phase—osteoporosis circumscripta)	

Figure 1-16 Types of matrix: osteoblastic. The matrix of a typical osteoblastic lesion is characterized by the presence of either fluffy, cotton-like densities within the medullary cavity, such as in this case of osteosarcoma of the distal femur **(A),** by the presence of the wisps of tumor-bone formation, like in this case of osteosarcoma of the sacrum **(B),** or by the presence of a solid sclerotic mass, such as in parosteal osteosarcoma **(C).**

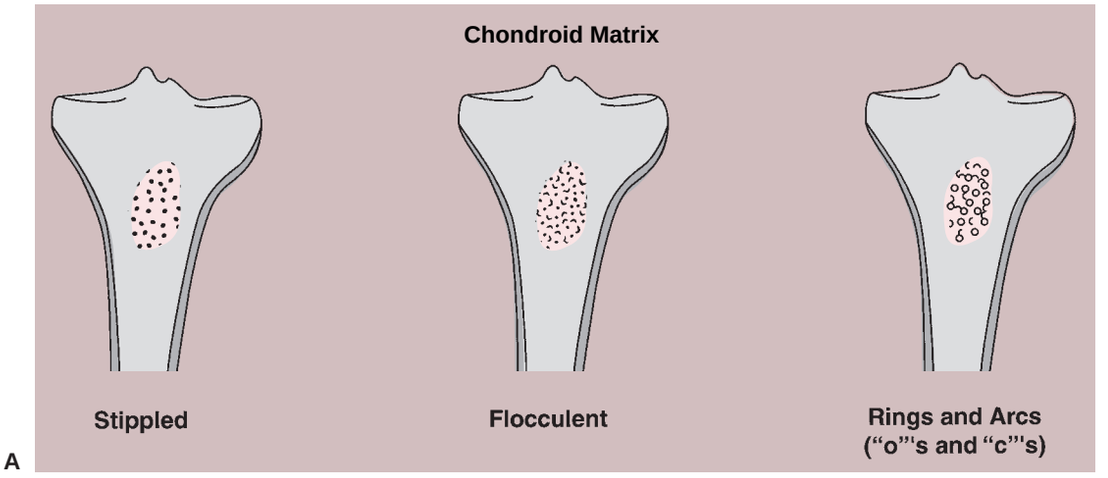

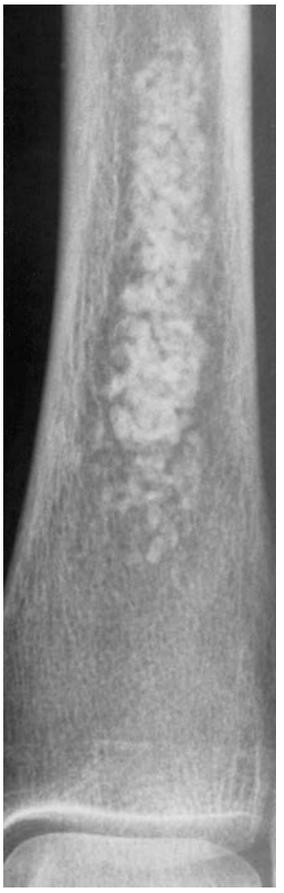
B


C

Figure 1-17 **Types of matrix: chondroid. A:** Schematic representation of various appearances of chondroid matrix calcifications. (Modified from Sweet DE, Madewell JE, Ragsdale BD. Radiologic and pathologic analysis of solitary bone lesions. Part III. Matrix patterns. *Radiol Clin North Am* 1981;19:785–814.) **B:** Enchondroma displays a typical chondroid matrix. **C:** Chondrosarcoma with characteristic chondroid matrix.

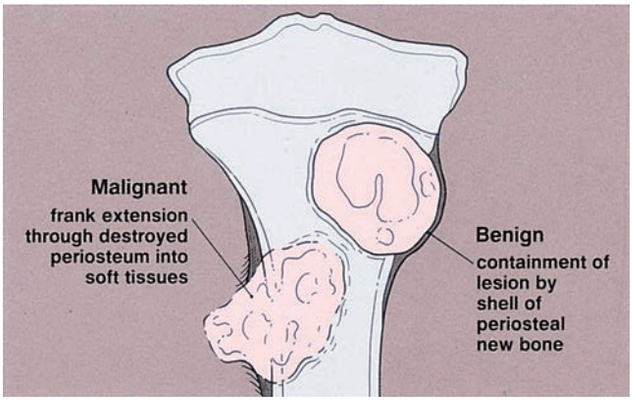

Figure 1-18 Soft tissue mass. Radiographic features of soft tissue extension characterizing malignant or aggressive bone lesions and benign processes.

Soft Tissue Mass

With few exceptions—giant cell tumor, aneurysmal bone cyst, and desmoplastic fibroma among the more common examples—benign bone tumors usually do not have an associated soft tissue mass, which is an invariable feature of many advanced malignant and aggressive lesions (94) (Fig. 1-18). Nevertheless, it is important to note that some nonneoplastic conditions also manifest with a soft tissue component (e.g., osteomyelitis). In such cases, however, the associated mass is usually poorly defined and the fatty tissue layers appear obliterated. This is in sharp contrast to the soft tissue extensions typical of malignant processes, in which a defined mass extends through the destroyed cortex but the tissue planes are usually intact.

A bone lesion associated with a soft tissue mass should prompt the question of which came first. Is the soft tissue lesion an extension of a primary bone tumor, or is it a primary soft tissue tumor invading bone? Some clues may help to answer this question, but these observations are by no means absolute (Fig. 1-19). A large soft tissue mass with a smaller bone lesion usually indicates secondary bone involvement. That said, it is worth noting that Ewing sarcoma and less commonly other malignant tumors may exhibit a large soft tissue mass accompanying a small primary bone malignancy. Another clue to help determine the primary malignancy may be found in the periosteal response. Primary soft tissue tumors adjacent to bone usually destroy the neighboring periosteum without eliciting a periosteal response. Primary bone malignancies, however, typically prompt a periosteal

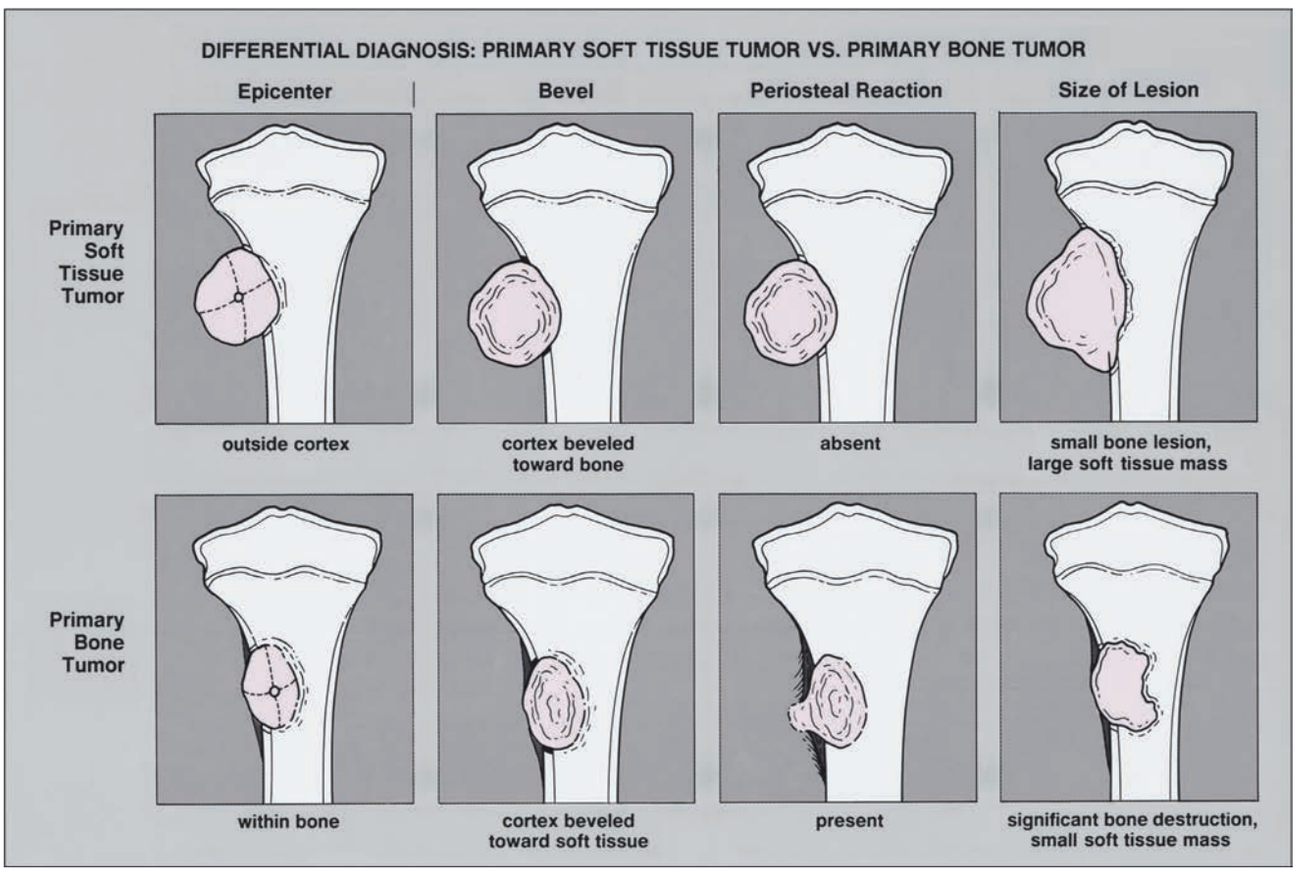

Figure 1-19 Differential diagnosis of soft tissue mass. Certain radiographic features of bone and soft tissue lesions may help differentiate a primary soft tissue tumor invading the bone from a primary bone tumor invading soft tissues. (From Greenspan A. *Orthopedic imaging,* 4th ed. Philadelphia: Lippincott Williams & Wilkins, 2004.)

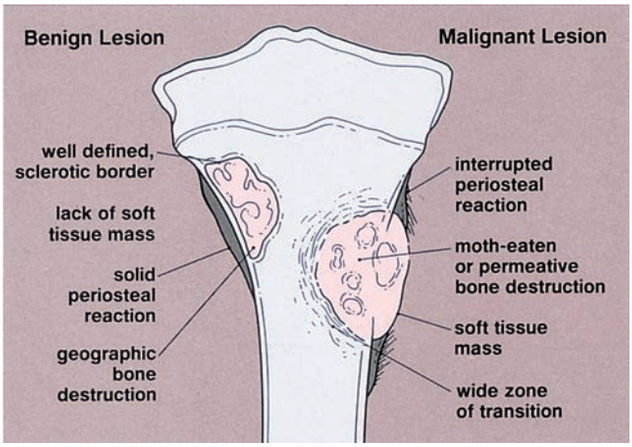

Figure 1-20 **Radiographic features that may help differentiate benign from malignant lesions.**

reaction when they grow into the cortex and extend into adjacent soft tissues (69,133,160).

Benign Versus Malignant Nature

Although it is sometimes very difficult to establish a lesion as benign or malignant by radiography alone, the clusters of features that can be gathered from radiographs can help in favoring one designation over the other (Fig. 1-20). Benign lesions usually have well-defined sclerotic borders and exhibit a geographic type of bone destruction; the periosteal reaction is solid and uninterrupted, and there is no soft tissue mass. In contrast, malignant tumors often exhibit poorly defined borders with a wide zone of transition; bone destruction appears in a moth-eaten or permeative pattern, and the periosteum shows an interrupted, sunburst, or onion-skin reaction with an adjacent soft tissue mass. It should be kept in mind, however, that some benign lesions may also exhibit aggressive features (Table 1-4).

Scintigraphy (Radionuclide Bone Scan)

The radionuclide bone scan is an indicator of mineral turnover. Because there is usually enhanced deposition of bone-seeking radiopharmaceutical agents in areas undergoing change and repair, a bone scan is useful in localizing tumors and tumor-like lesions in the skeleton (58). This is particularly true in such conditions as fibrous dysplasia, Langerhans cell histiocytosis, and metastatic cancer, in which more than one lesion is encountered. Technetium-99m methyl diphosphonate (MDP) scans are used primarily to determine whether a lesion is monostotic or polyostotic. Such a study is therefore essential in staging a bone neoplasm. It is important to remember that although the degree of abnormal uptake may be related to the aggressiveness of the lesion, this does not correlate well with the histologic grade (Fig. 1-21).

Radionuclide bone scan also plays an important role in localizing small lesions such as osteoid osteoma, which may not always be visible on radiography (Fig. 1-22). Although skeletal scintigraphy is a highly sensitive method for detection of bone neoplasms, its specificity is low. In most instances it cannot distinguish benign lesions from malignant tumors, because increased blood flow with increased isotope deposition and increased osteoblastic activity take place in both benign and malignant conditions. Nevertheless, it can sometimes achieve such differentiation in benign lesions that do not absorb the radioactive isotope. In addition, the radionu-

Table 1-4 **Benign Lesions with Aggressive Features**

Lesion	Radiographic Presentation	Lesion	Radiographic Presentation
Osteoblastoma (aggressive)	Bone destruction and soft tissue extension similar to osteosarcoma	Osteomyelitis	Bone destruction, aggressive periosteal reaction. Occasionally, features resembling osteosarcoma, Ewing sarcoma, or lymphoma
Desmoplastic fibroma	Expansive, destructive lesion, frequently trabeculated, mimics fibrosarcoma and chondrosarcoma	Langerhans cell histiocytosis	Bone destruction, aggressive periosteal reaction. Occasionally, features resembling Ewing sarcoma
Periosteal desmoid	Irregular cortical outline, mimics osteosarcoma or Ewing sarcoma	Pseudotumor of hemophilia	Bone destruction, periosteal reaction, occasionally mimics malignant tumor
Giant cell tumor	Occasionally, aggressive features such as osteolytic bone destruction, cortical penetration, and soft tissue extension	Myositis ossificans	Features of parosteal or periosteal osteosarcoma, soft tissue osteosarcoma, or liposarcoma
Aneurysmal bone cyst	Soft tissue extension, occasionally mimics malignant tumor such as telangiectatic osteosarcoma	Brown tumor of hyperparathyroidism	Lytic bone lesion, resembling malignant tumor

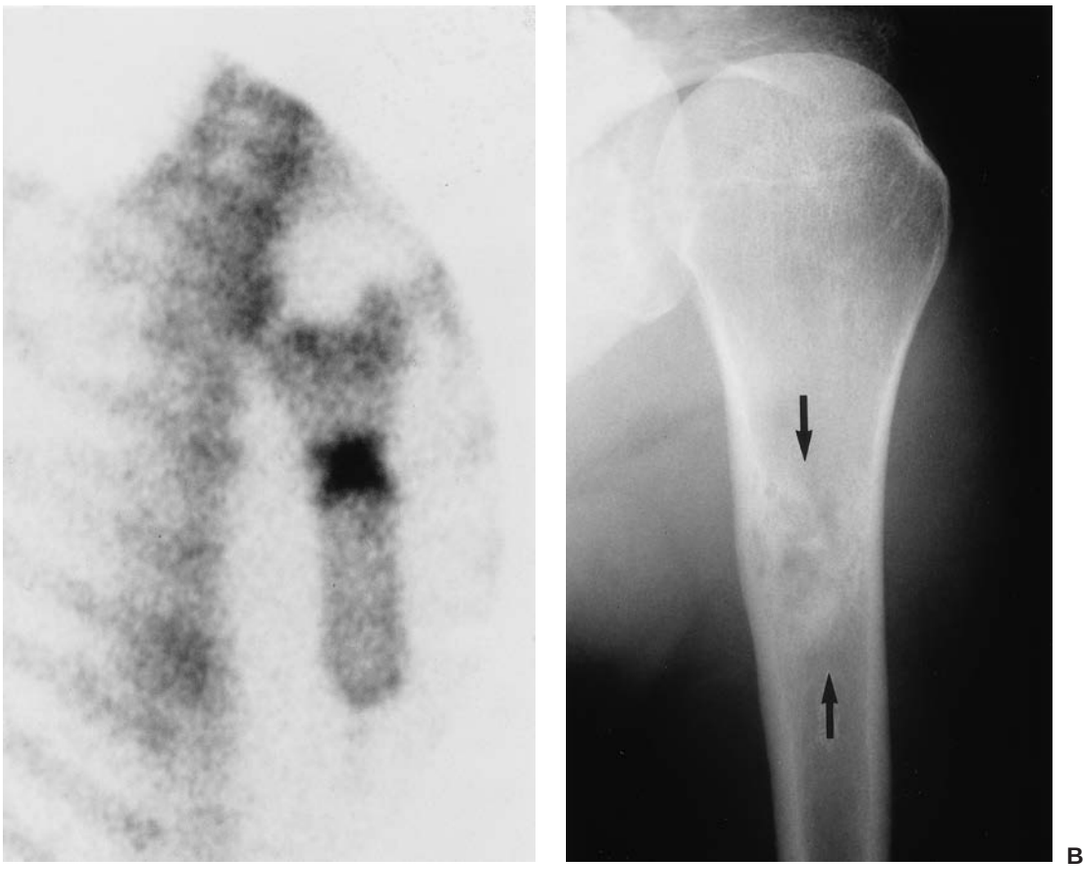

Figure 1-21 Scintigraphic activity. A: Radionuclide bone scan shows markedly increased uptake of radiotracer in the proximal humerus in a 26-year-old woman suspected of developing a malignant tumor. **B:** Anteroposterior radiograph shows, however, a benign-appearing lesion with sclerotic border (*arrows*), consistent on excision biopsy with healing benign fibrous histiocytoma. (Reprinted with permission from Greenspan A. *Orthopedic imaging,* 4th ed. Philadelphia: Lippincott Williams & Wilkins, 2004.)

clide bone scan is sometimes useful for differentiating multiple myeloma, which usually shows no significant uptake of the tracer, from metastatic bone cancer, which usually does. Scans using Ga-67 may show uptake in a soft tissue sarcoma and may help to differentiate a sarcoma from a benign soft tissue lesion.

Imaging with thallium-201 chloride has recently been tried in the diagnosis of bone and soft tissue lesions (26,44,112,171,190,206). Although the role of this technique for staging of bone tumors and for differentiation of benign from malignant lesions is limited, thallium-201 scintigraphy appeared useful in detection of primary and metastatic neoplasms, such as synovial sarcoma (112) and some of the cartilaginous tumors (29). Furthermore, the combined use of Tl-201 and pentavalent dimercaptosuccinic acid (DMSAV) functional nuclear scanning proved to be promising in the differential diagnosis of benign and malignant cartilage lesions and their grading (29).

The essential factors in the evaluation of a bone lesion are intra- and extraosseous extension, and presence (or absence) of metastases. Although radiography can yield significant information about tumor extension, skeletal scintigraphy is an indispensable technique for evaluating whether a tumor has spread beyond its site of origin (12,15,28,62,152,194). Radionuclide bone imaging better demonstrates the extent of intramedullary involvement by tumor than radiography, but it tends to show a larger than actual area of extension because the radiopharmaceutical also localizes to areas of hyperemia and edema adjacent to the tumor (15). Therefore, bone scans are not adequate for evaluating the exact level of intramedullary invasion. However, scintigraphy has no competitor (except for MRI) for identifying additional remote skeletal lesions, so-called skip lesions, and intraosseous metastases (55).

Scintigraphy and MRI or CT are truly complementary examinations that provide quite different staging information for the patient who presents with a bone tumor that requires biopsy (167–169). The main role of scintigraphy is not so much for local staging as for evaluating the remainder of the skeleton. Although scintigraphy provides information on the intraosseous extent of disease, it cannot entirely be relied on for

Figure 1-22 Effectiveness of skeletal scintigraphy. A: Anteroposterior radiograph of the left hip of a 16-year-old boy with a typical history of osteoid osteoma is equivocal, although there is the suggestion of abnormal radiolucency in the supraacetabular portion of the ilium. **B:** Radionuclide bone scan shows an increased uptake of radiopharmaceutical agent (*arrow*) corresponding to questionable radiolucency seen on radiography. Osteoid osteoma was diagnosed on excision biopsy. (Reprinted with permission from Greenspan A. *Orthopedic imaging,* 4th ed. Philadelphia: Lippincott Williams & Wilkins, 2004.)

local extent of the lesion [because of the augmented uptake that has been described in osteosarcomas (28,79)], its inability to match MRI in differentiating normal from abnormal marrow, and its inability to adequately demonstrate extracompartmental disease. Increased uptake of radionuclides is highly nonspecific. Any pathologic process in bone that leads to new bone formation (reactive or tumor bone), increased blood flow, or bone turnover, will show increased radionuclide uptake (58). Therefore, a bone scan is usually not reliable for identifying the specific type of tumor or for differentiating malignant from benign processes. Despite these factors, scintigraphy is still an important technique for evaluation of solitary bone tumors. Because scintigraphy is the most sensitive examination for imaging the entire skeleton, it should always be performed to determine whether skeletal involvement is solitary or multiple. Metastases are the most common malignant tumors of bone and can frequently present as a solitary abnormality. In the pediatric age group, as in adults, metastases may mimic solitary tumors of bone. Metastatic neuroblastoma and leukemia may resemble true solitary lesions such as Ewing sarcoma, Langerhans cell histiocytosis, and acute osteomyelitis. Because synchronous and delayed skeletal metastases may occur, scintigraphy is recommended at initial presentation and in follow-up of patients after extirpation of primary Ewing tumor (62). Scintigraphy can suggest the presence or absence of disseminated skeletal disease. In the proper clinical setting its appearance can be quite specific for the diagnosis of osteoid osteoma (172) (see Fig. 2-35).

Positron Emission Tomography

PET is a diagnostic imaging technique that allows identification of biochemical and physiologic alterations in the body and assesses the level of metabolic activity and perfusion in various organ systems. The process produces biologic images based on detection of gamma rays that are emitted by a radioactive substance, such as ^{18}FDG. One of the main applications of this technique is in oncology, including detection of primary and metastatic tumors and recurrences of the tumors after treatment (Fig. 1-23). In fact, PET has been found to be more sensitive than CT and MRI in this respect. Although some promising results have been reported using this technique (8), detection of bone marrow involvement is still controversial, because physiologic bone marrow uptake can be observed on ^{18}FDG PET images. Moreover, although highly sensitive, PET scanning has relatively low specificity because FDG may also accumulate in benign aggressive and inflammatory lesions.

Recently, Zhang et al. conducted investigations of the utility of ^{11}C-methionine (MET) PET in the imaging of chordoma (215). Their study has demonstrated that MET PET is feasible for imaging of chordoma, showing a sensitivity of 80% in the visualization of all tumors, and 100% for the recurrent lesions.

Computed Tomography and Magnetic Resonance Imaging

Both CT and MRI are highly accurate for determining the presence of neoplasm within the cortex, trabecular

bone, or marrow cavity, as well as soft tissue invasion by a tumor (98,150,188,193,199,212,217). Although CT by itself is rarely helpful in making a specific diagnosis, it can provide a precise evaluation of the extent of a bone lesion and may demonstrate breakthrough of the cortex and involvement of surrounding soft tissues (Fig. 1-24). Moreover, CT is very helpful in delineating a bone tumor in a complex anatomic structure such as scapula, pelvis, or sacrum (Fig. 1-25). At times, the three-dimensional reformation of CT images is used to better and more comprehensively demonstrate the tumors (25,53, 97). This technique can be useful in depicting the surface lesions of bone, such as osteochondroma (Fig. 1-26; see also Fig. 3-50), periosteal chondroma, parosteal osteosarcoma, or juxtacortical chondrosarcoma. The use of CT versus MRI is based on the radiographic findings: if there is no definite evidence of extension of osseous tumor into the soft tissues, then CT is preferred for detecting subtle cortical invasion and periosteal reaction, while providing an accurate means of determining the intraosseous extension of the neoplasm. If, however, the radiographs suggest cortical destruction and soft tissue mass, then MRI would be the more desirable modality because it provides an excellent soft tissue contrast and can determine the extraosseous extension of the tumor much better than CT. In addition, MRI provides valuable information regarding the intraosseous extent of neoplasms based on its multiplanar imaging ability (sagittal, coronal, axial, and oblique) and lack of beam-hardening artifacts from cortical bone. Because of superior ability to characterize soft tissue masses, MRI has distinct advantages over CT (11,31,216) (Fig. 1-27).

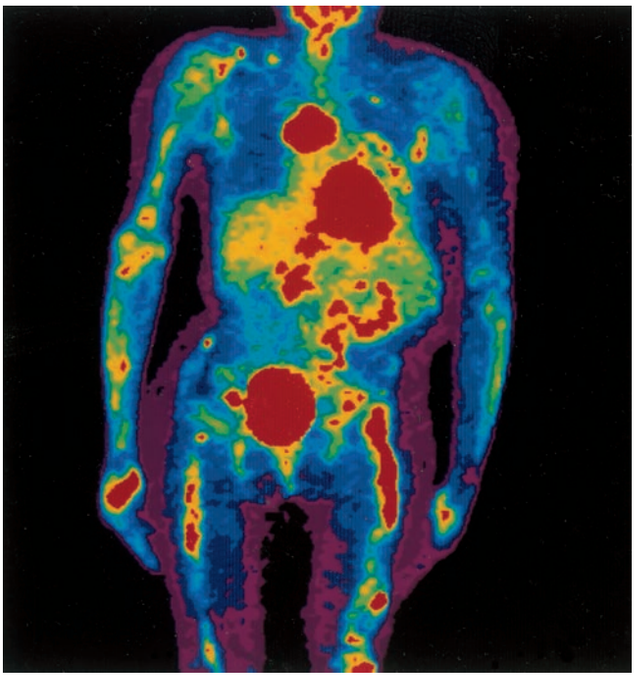

Figure 1-23 Positron emission tomography (PET) scan. ^{18}FDG whole body PET scan of a 37-year-old woman with known fibrous dysplasia shows multiple skeletal deformities of the long bones. Red areas represent large hypermetabolic foci. (Courtesy of Drs. Frieda Feldman and Ronald van Heertum, New York, New York.)

A number of pulse sequences can be used to evaluate musculoskeletal tumors (66,154). These include spin-echo (SE) sequences, inversion recovery (IR) sequences, short time inversion-recovery (STIR) sequences, gradient echo (GRE) sequences, and fast T2- or fat-suppressed T2-weighted sequences (11,43,65,158,183). SE sequences are the most effective for identification and staging of most skeletal tumors (10,216). The signal intensity for normal tissues is predictable using these sequences. On T1-weighted images, fat and bone marrow have a high signal intensity that changes to intermediate intensity on T2 weighting. Muscles have intermediate signal intensity on both T1 and T2 sequences. Cortical bone and fibrocartilage have low signal on both sequences. Fluid has intermediate signal on T1-weighted and high signal intensity on T2-weighted images (Table 1-5). Most bone tumors have increased T1 and T2 relaxation times compared with normal tissue and therefore are imaged as areas of low or intermediate signal intensity on T1-weighted SE sequences and high signal intensity on T2-weighted sequences (11,63,216). T1-weighted SE sequences enhance tumor contrast with bone, bone marrow, and fatty tissue, whereas T2-weighted SE or T2-weighted gradient echo images enhance tumor contrast with muscle and accentuate peritumoral edema (73,132,151,191,195,207) (Fig. 1-28).

Several investigators have stressed the advantage of contrast enhancement of MR images using intravenous injection of gadopentate dimeglumine [gadolinium diethylenetriaminepentaacetic acid (Gd-DTPA)] (74,178). This paramagnetic contrast enhancement on conventional T1-weighted sequences decreases the T1 relaxation time in tumor tissue causing the lesion to be of higher signal intensity (hence making the demarcation of the tumor more obvious) (Fig. 1-29). In particular, enhancement was found to give better delineation of tumor in richly vascularized parts, in compressed tissue immediately surrounding the tumor, and in atrophic but richly vascularized muscle (153). Both static and dynamic Gd-DTPA studies show significant promise for evaluation of musculoskeletal tumors (47,98,208). Areas that demonstrate contrast enhancement on T1 weighting are typically more vascular, whereas those without enhancement usually represent necrotic tissue (47). In addition, utilization of a chemical shift or fat suppression technique is even more effective (128) because the fat signal becomes markedly suppressed, whereas the abnormal contrast-enhanced tumor displays a high signal intensity (127,197,198). This combination improves the interface between tumor and peritumoral edema, the interface between tumor and reactive zone, and the interface between tumor and adjacent muscle (179,197,198).

Figure 1-24 Effectiveness of computed tomography (CT) scanning. A: Conventional radiograph shows destructive changes in the proximal diaphysis of the left fibula (*arrows*) of a 12-year-old boy. **B:** CT scan demonstrates involvement of the bone marrow of the fibula (*arrow*) and extension of the tumor (which proved to be a Ewing sarcoma) into the soft tissues (*arrowheads*).

Coronal-plane MR images, in particular, are often superior to axial CT scans in providing details of extra- and intramedullary tumor extent and its relationship to surrounding structures (61). Combining axial and coronal plane imaging has also been helpful in assessing important vascular structures adjacent to tumors. In addition, MRI offers better visualization of tissue planes surrounding a lesion and can evaluate neurovascular involvement without the use of intravenous contrast (45). Particularly in tumors of the extremities, the ability of MRI to demarcate normal from abnormal tissue more sharply than CT can reliably delineate the spatial boundaries of tumor masses, encasement and displacement of major neurovascular bundles, and the extent of joint involvement (1,100).

In several respects, however, CT unquestionably rivals MRI. MR images do not clearly depict calcifications in the tumor matrix or allow it to be characterized as readily as CT. In fact, large amounts of calcification and ossification have occasionally gone almost undetected by MRI (195). In addition, MRI demonstration of cortical destruction and periosteal reaction is less satisfactory than that of CT or even of radiography (67,191). Although neither technique is usually suitable for establishing the precise nature of a bone tumor (except perhaps the characteristic MRI features of intraosseous lipoma and hemangioma), much faith has been placed in MRI in particular as a method capable of distinguishing benign from malignant lesions (16,47,76,93,109). An overlap between the classic characteristics of benign and malignant tumors is often observed (110). Moreover, some malignant bone tumors can appear misleadingly benign on MR images and, conversely, some benign lesions may exhibit a misleadingly malignant appearance (36,110). Attempts to formulate precise criteria for correlating MRI findings with histologic diagnosis have been largely unsuccessful (195). Tissue characterization on the basis of MRI signal intensities is still unreliable. Because of the wide spectrum of bone tumor composition and their differing histologic patterns, as well as in tumors of similar histologic diagnosis, signal intensities of histologically different tumors may overlap or there may be variability of signal intensity in histologically similar tumors. MRI is sensitive for delineating the extent of disease but, unfortunately, is relatively nonspecific (164,165,191).

Pathology

The task of categorizing an osseous lesion as benign or malignant is even more complex for the pathologist than for the radiologist. In bone tumor pathology, about 70 entities must be differentiated, most of them representing a very low incidence. In fact, primary malignant bone tumors comprise only 1% of all malignancies, and about half of these represent multiple myeloma. Accordingly, the diagnostic density, even in a large institution, may not be sufficient to ensure diagnostic security. Therefore, an opinion from a bone

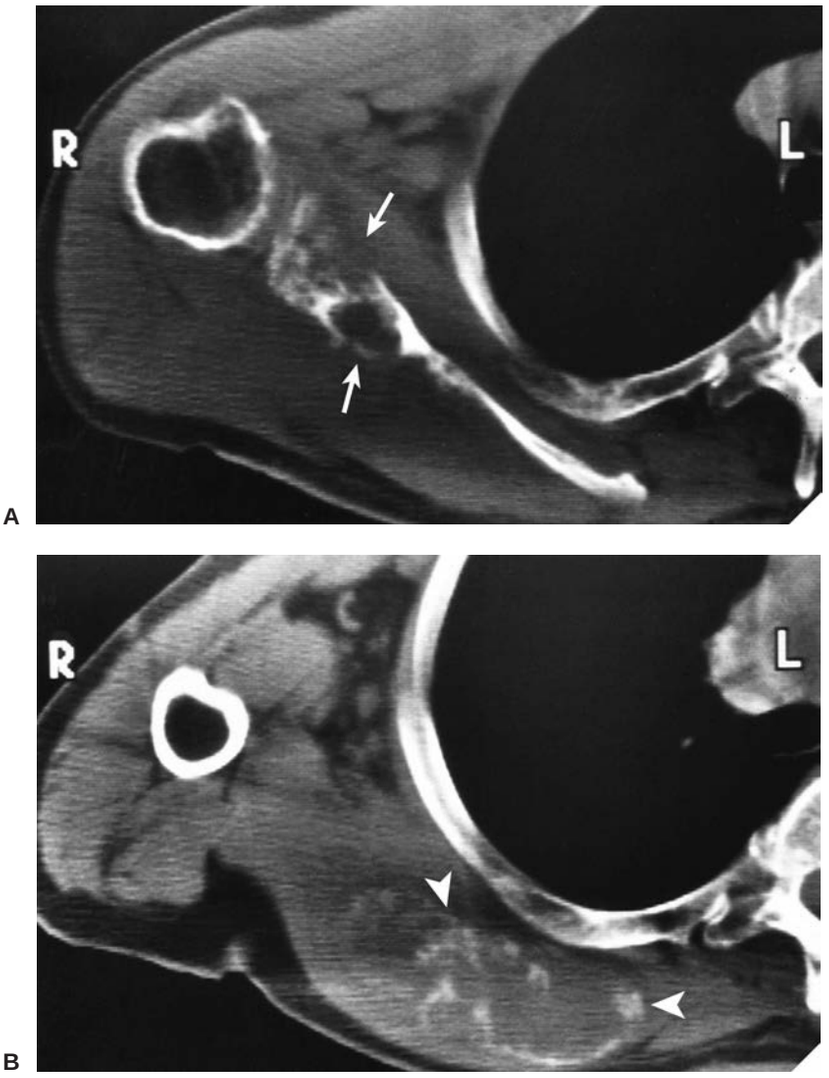

Figure 1-25 Effectiveness of computed tomography (CT) scanning. Standard radiographs (not shown here) were ambiguous in this 70-year-old man with a palpable mass over the right scapula. However, two CT sections show a destructive lesion of the glenoid portion and body of the scapula (*arrows*) **(A)**, with a large soft tissue mass containing chondroid calcifications and extending to the rib cage (*arrowheads*) **(B)**. The lesion proved to be a chondrosarcoma.

tumor reference center should be obtained in all doubtful cases. For the pathologist, it is mandatory to view at least the radiographs (and the cross-sectional studies of tumors affecting the spine, pelvis, and shoulder girdle) and to consider all the radiologic criteria (see previous discussion), together with the data supplied by the clinician. Ideally, the pathologist should also consult with both the radiologist and the orthopedic surgeon. Although it may be obvious to a clinician that a child with a rock-hard, tender, 15-cm swelling of the femur almost undoubtedly has a tumor, a 4-mm sampling of tissue from the same lesion, unaccompanied by a history and radiologic studies, is fraught with diagnostic risk (68). Without consideration of all available correlative measurements before an attempt is made to interpret histologic sections, there is no assurance that a biopsy specimen is representative of the lesion or, in fact, that the actual abnormality has been sampled. This is particularly true for chondroblastic tumors, in which benign tissue may be dispersed within the malignant portion of a tumor, and vice versa.

Basic Techniques and Decalcification

After results of the necessary clinical correlation studies are considered, the histologic diagnosis is rendered. For technical details of the different staining procedures mentioned later, the reader is referred to standard textbooks of histochemistry and histotechnology (6,17,78,157). The tumor cells and their arrangement, as well as the intercellular matrix

Text continues on page 28

A

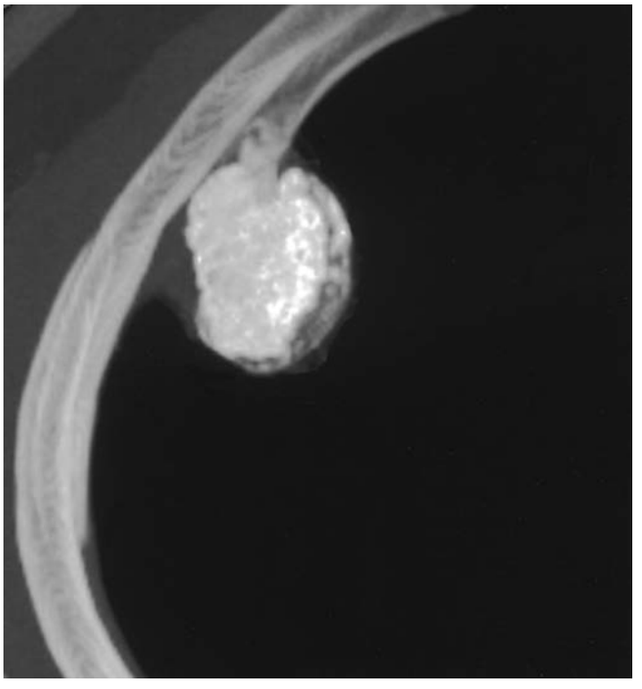

B

C

Figure 1-26 Effectiveness of three-dimensional computed tomography (CT). A: Conventional CT section through the chest shows an osteochondroma at the site of the anterolateral portion of the right fourth rib *(arrow)*. It is difficult to determine if the lesion is sessile or pedunculated. **B:** Three-dimensional CT in maximum intensity projection (MIP) allows one to characterize the internal architecture of the lesion and delivers a much more informative image of osteochondroma. Note typical chondroid matrix of the tumor. **C:** Three-dimensional CT in shaded surface display (SSD) renders better conspicuity of the lesion; the pedicle of osteochondroma (*arrow*) is now clearly demonstrated.

A

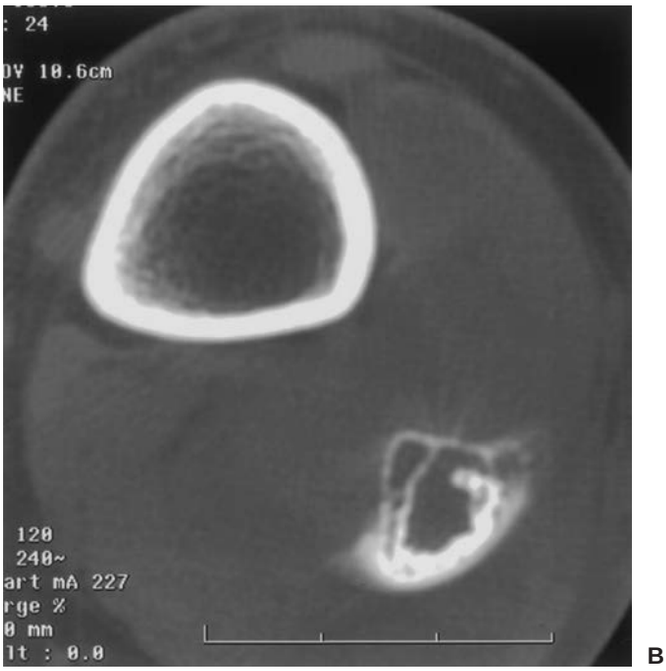

B

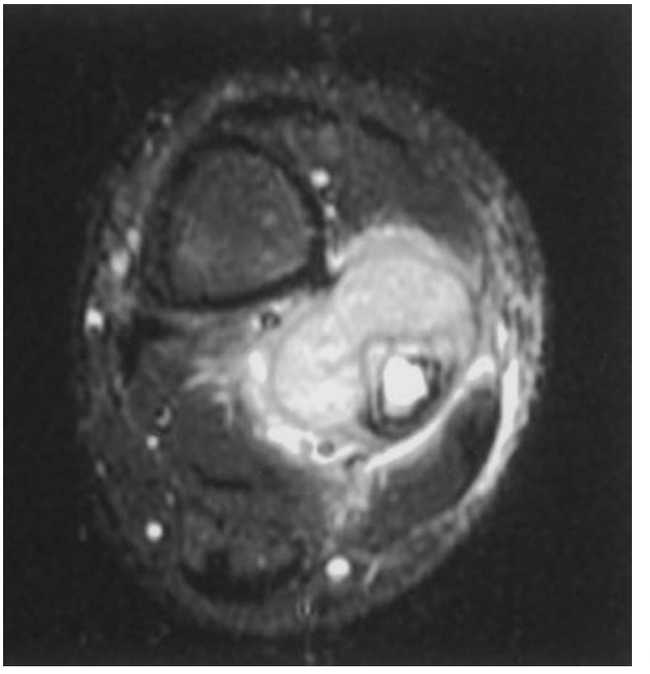

C

Figure 1-27 Effectiveness of magnetic resonance imaging (MRI) versus computed tomography (CT). A: Anteroposterior radiograph of the lower leg of a 14-year-old boy with Ewing sarcoma of the distal fibular diaphysis shows moth-eaten destruction of the bone and aggressive periosteal reaction. Soft tissue mass is not well demonstrated. **B:** CT scan effectively demonstrates cortical destruction of the fibula and periosteal reaction, but the soft tissue mass is not well characterized. **C:** Axial T2-weighted fat-suppressed MRI clearly shows a large soft tissue mass adjacent to the osseous tumor.

Figure 1-28 Magnetic resonance imaging (MRI): T1 versus T2 weighting. Sagittal **(A)** and axial **(B)** spin-echo T1-weighted MRIs of a 29-year-old woman with malignant fibrous histiocytoma in the left tibia show excellent demarcation of low-signal-intensity tumor from high-signal-intensity bone marrow. **C:** Axial spin-echo T2-weighted MRI shows to better advantage the demarcation between the surrounding soft tissues and a heterogeneous-high-signal-intensity tumor that is breaking through the cortex.

Table 1-5 **Magnetic Resonance Imaging Signal Intensities of Various Tissues**

	Image	
Tissue	***T1-weighted***	***T2-weighted***
Hematoma, hemorrhage (acute, subacute)	High/intermediate	High
Hematoma, hemorrhage (chronic)	Low	Low
Fat, fatty marrow	High	Intermediate
Muscle, nerves, hyaline cartilage	Intermediate	Intermediate
Cortical bone, tendons, ligaments, fibrocartilage, scar tissue, air	Low	Low
Hyaline cartilage	Intermediate	Intermediate
Red (hematopoietic) marrow	Low	Intermediate
Fluid	Intermediate	High
Proteinaceous fluid	High	High
Tumors (generally)	Intermediate-to-low	High
Lipoma	High	Intermediate
Hemangioma	Intermediate (slightly higher than muscle)	High

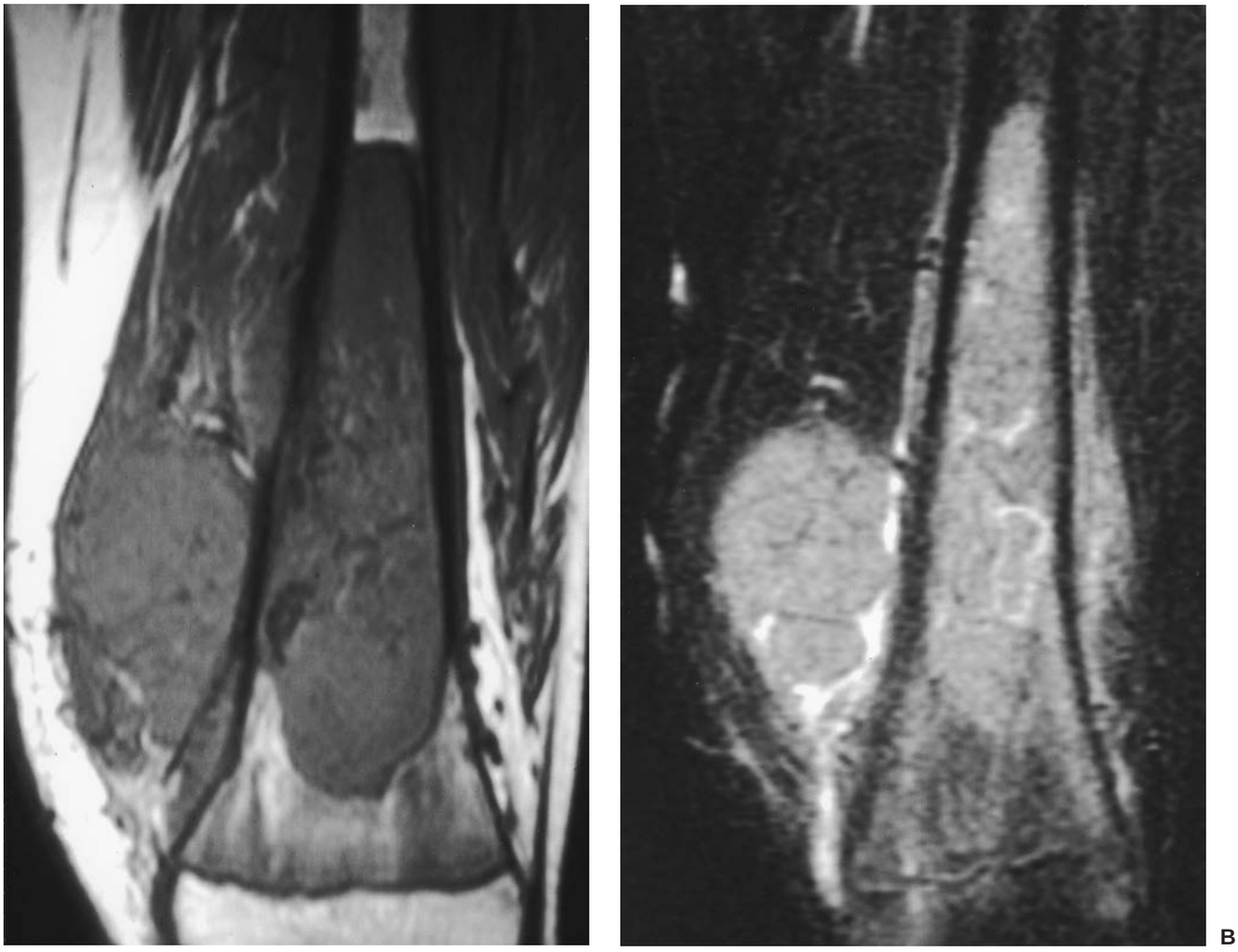

A B

Figure 1-29 Magnetic resonance imaging (MRI): contrast enhancement. A: Coronal T1-weighted MRI of a 14-year-old boy with osteosarcoma in the distal left femur shows a low-signal-intensity tumor in the bone marrow associated with a soft tissue mass. **B:** After intravenous administration of gadolinium (Gd-DTPA) there is a heterogeneous enhancement of both intramedullary tumor and soft tissue mass.

produced, are compared with the appearance of radiographs and other imaging studies to verify adequate and representative sampling. The histologic patterns are then compared and matched with similar or identical histologic patterns of known examples of bone tumors (200). For daily diagnostic requirements, standard hematoxylin and eosin (H&E) staining after decalcification is usually sufficient (Fig. 1-30). Only for some histochemical and immunocytochemical methods does previous decalcification represent an obstacle. Acidic decalcifiers such as formic acid (5%–10% solutions) are ordinarily used. These agents provide good results within a short period of time. Because formic acid is not as rapid a decalcifier as nitric acid, the tissue structure is well preserved and good staining for H&E is retained (185). Most immunohistochemical protocols can also be applied. However, genetic analyses are often seriously hampered. Decalcification by EDTA, a chelating agent, does not pose these problems but is much more time-consuming (181). However, its use in combination with ultrasound leads to a reduction in time (126). Recently developed automated techniques of EDTA decalcification combined with ultrasound allow much more rapid decalcification, at least for small samples such as core biopsies (38). An earlier method, introduced about 20 years ago, of embedding the bone specimen in plastic and cutting it without previous decalcification, which is necessary for histomorphometric purposes, does not substantially contribute to bone tumor diagnostics.

Special Stains and Enzyme Histochemistry

Among the special stains available is van Gieson stain, which is more commonly used in Europe. This stain helps to identify the presence and amount of collagen in bone and other connective tissues by staining it intensely red (Fig. 1-31). This method is particularly effective to identify osteoid, whose major component is type I collagen. Giemsa stain should be used in the differentiation of small, blue, round cell tumors, particularly the lymphomas (Fig. 1-32). It also intensely stains the arrest lines in the bone matrix, thus making apposition and reconstruction processes clearer in an H&E preparation. We have found it useful in the differentiation of bone and cartilage when both tissues are intermingled because of the metachromatic properties. The Alcian blue stain can be useful in a similar manner (Fig. 1-33). Reticulin fibers are usually stained with Gomori stain, which is helpful in the differentiation against collagen fibers (Fig. 1-34). We prefer the variation of this stain described by Novotny, in which the fibers stand out more clearly (Fig. 1-35). Periodic acid–Schiff (PAS) staining is effective in demonstration of glycogen in the cytoplasm (Fig. 1-36). Another helpful tool is enzyme histochemistry, in particular the demonstration of alkaline phosphatase as marker for osteoblasts (Fig. 1-37A) and acid phosphatase as marker for osteoclasts (Fig. 1-37B).

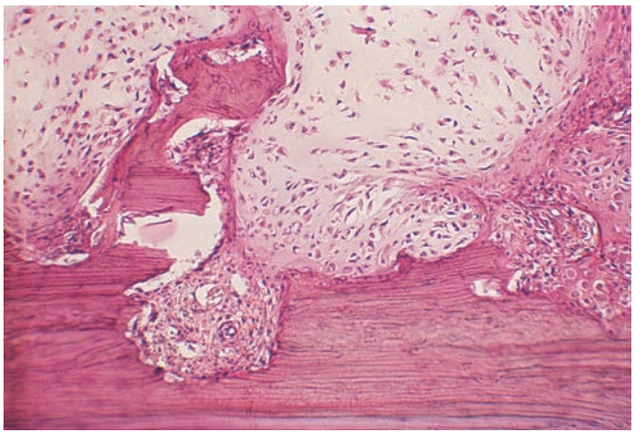

Figure 1-30 Hematoxylin and eosin (H&E) stain. Chondrosarcoma. The cortex of the femur (*bottom*) shows large resorption lacunae (*center and right*) with cartilaginous tumor tissue invading the bone. Some osteoclasts that created the excavations are still visible (*center*). The cartilage stains pink; the bone stains red (H&E, original magnification ×100).

Immunohistochemistry

A more recent method is immunohistochemistry (IHC), which demonstrates by immunologic methods specific antigens that serve as markers on the cell surface and its inner structures (60,130,174). By choosing the appropriate detection methods, including antigen retrieval techniques, almost any available antibody can be used to label a cell or a tissue (34,41). Studies using IHC are extremely helpful in differentiating among tissues that have similar morphology or whose histologic origins are uncertain. IHC can identify the antigenic factors in cells that would not other-

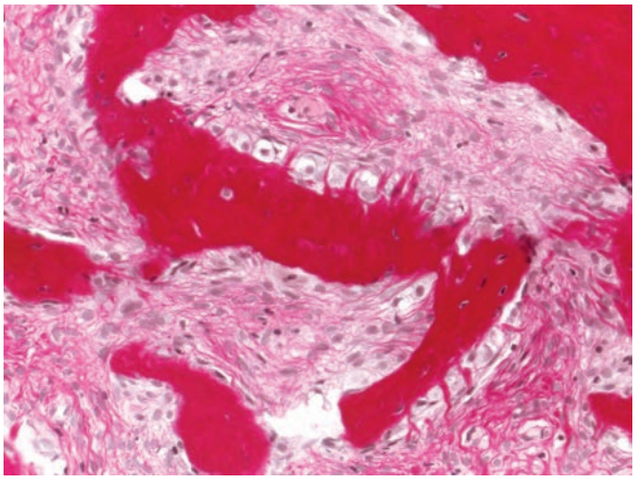

Figure 1-31 Van Gieson stain. Fibrous dysplasia. Note irregular bony trabeculae typical for this disorder. Collagenous fibers are stained intensely red; particularly Sharpey fibers are highlighted in perpendicular arrangement to the trabecular surface (van Gieson, original magnification ×200).

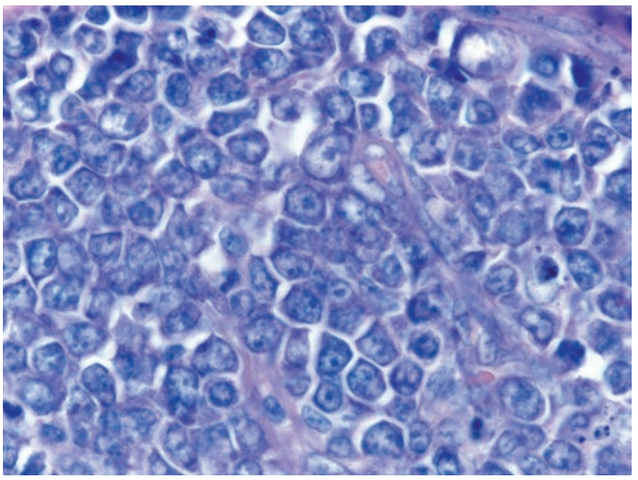

Figure 1-32 Giemsa stain. Diffuse large B-cell lymphoma. DNA, RNA, and basophilic cytoplasmic components are stained purple to grey-blue, helping to identify nuclear details of lymphoma cells (Giemsa, original magnification ×630).

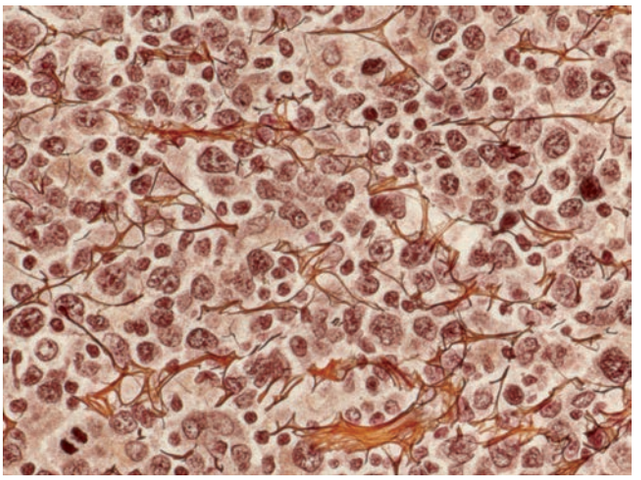

Figure 1-34 Gomori stain. Diffuse large B-cell lymphoma. Reticulin fibers appear as fine dark-brown to black network encircling lymphoma cells in a bone marrow biopsy specimen (Gomori, original magnification ×630).

wise be evident in histologic sections stained by routine methods. Nevertheless, although highly specific antibodies have been developed, as well as sensitive systems for immune and enzymatic detection, there remain problems with false-positive and false-negative results (60). IHC relies on the use of enzyme-linked antibodies for detection of tissue antigens. The enzyme antibody converts a colorless substrate into a stained product that is precipitated on the slide at the site of the reaction. Continuing development of techniques for IHC has led to the use of enzyme labeling with alkaline phosphatase and peroxidase. Labeling with colloidal gold is also used in IHC reactions for both light and electron microscopy. However, the avidin-biotin-complex (ABC) method has now become the most sensitive and widely used technique for immunohistochemical staining (60).

For diagnostic purposes, the application of IHC in bone tumor pathology is necessary only in a limited number of cases, mainly Ewing tumor family [Ewing sarcoma and primitive neuroectodermal tumor (PNET)], hematopoietic tumors and histiocyte disorders, vascular tumors, chordoma, adamantinoma of long bones and, of course, metastatic disease. The IHC reaction pattern that characterizes a lesion is discussed in the appropriate chapters.

It cannot be overemphasized that a positive immunoreaction is not a substitute for a diagnosis of a

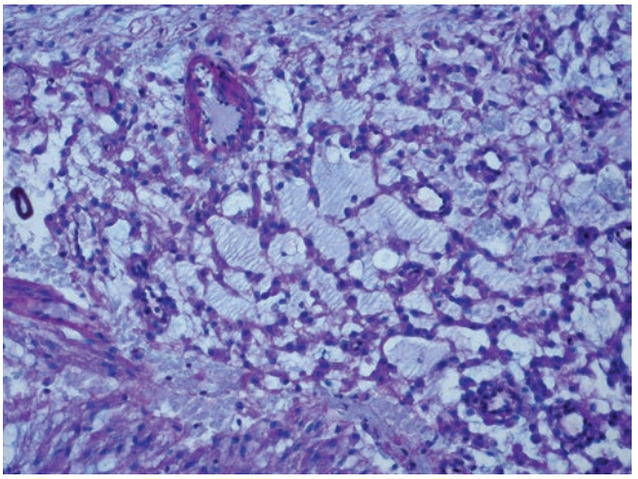

Figure 1-33 Alcian blue–periodic acid–Schiff (PAS) stain. Extraskeletal myxoid chondrosarcoma. Alcian-positive pale blue mucin pools contain acidic glycoproteins. Basement membrane material of capillaries (*upper left*) stains pink with PAS (original magnification ×200).

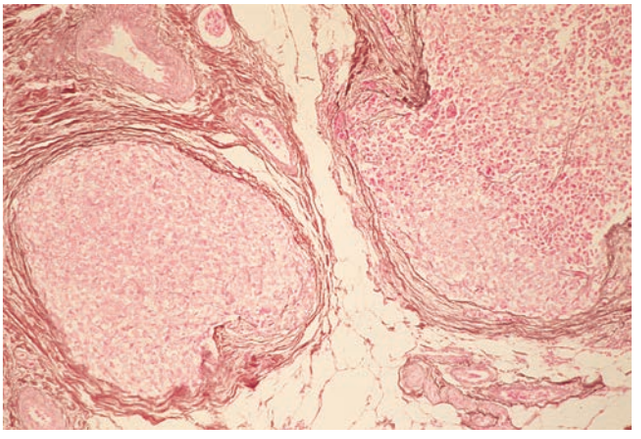

Figure 1-35 Novotny stain. Ewing sarcoma. Reticulin fibers that stain black are absent within tumor cell areas, thus excluding diagnosis of malignant lymphoma and small cell osteosarcoma (Novotny, original magnification ×12).

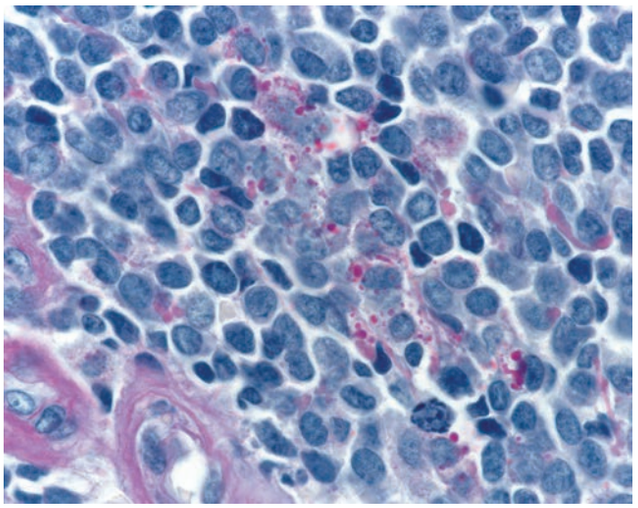

Figure 1-36 Periodic acid–Schiff (PAS) stain. Ewing sarcoma. Glycogen droplets (*center*) and glycoprotein-containing basement membrane material of capillaries (*bottom left*) stain pink to red. Because glycogen is water-soluble, it may partly be removed by formalin fixation (PAS, original magnification ×630).

specific bone tumor, which should be established only by taking into account the additional clinical, radiologic, and histologic findings. The most commonly used antibodies are briefly described in the following sections.

Antibodies Against Intermediate Filaments

Intermediate filaments (IFs) are structural proteins with a diameter of 8 to 10 nm (nanometers) and a molecular weight of 40 to 110 KD (kilodalton). Together with microtubuli (24 nm) and microfilaments (6 nm), the IFs form the cytoskeleton (116). IFs can be separated into five distinct types on the basis of sequence identify and tissue distribution (27). For diagnostic purposes, the most important members of the IF family are the cytokeratins (CKs), desmin, neurofilaments, glial fibrillary acidic protein (GFAP), and vimentin.

With the use of two-dimensional gel electrophoresis, 20 different CKs have been identified and numbered. They constitute two groups of basic (CK 1–8) and acidic (CK 9–20) CKs that form heterodimers (27,56,129). CKs are found predominantly in epithelial cells but have also been detected in other tissues. Therefore, a positive immunoreaction for CKs does not unequivocally prove the epithelial nature of a tumor under investigation. In bone tumors, CKs are typically expressed in adamantinomas of long bones, in chordoma (Fig. 1-38), in osteofibrous dysplasia, in epithelioid hemangioendothelioma, and in metastases of extraosseous cancer. However, "aberrant" expression can be found in almost all types of nonepithelial tumors, including osteosarcoma (142).

Vimentin is present in all mesenchymal and some epithelial cells. Its IHC detection in mesenchymal tumors is rarely of diagnostic value (34).

Desmin is present in all muscle tissues, stabilizing the contractile apparatus. It is found in both smooth muscle and skeletal muscle tumors and also in lesser amounts in myofibroblasts (175). Antibodies to desmin are used mainly for the differential diagnosis of spindle cell tumors (161).

Neurofilaments (NFs) are present in neural cells in three different forms: high molecular weight NF-H (200 KD), medium weight NF-M (160 KD), and low weight NF-L (68 KD). They can be detected in small amounts in tumors of the Ewing family, such as PNETs or classical Ewing sarcomas, and especially in neuroblastomas (149,201).

GFAP is present in glial cells and is almost never used in studies of bone tumor pathology (162).

Antibodies Against Hematopoietic and Lymphoid Cells

Antibodies against hematopoietic and lymphoid cells are widely used in the diagnosis of lymphomas and

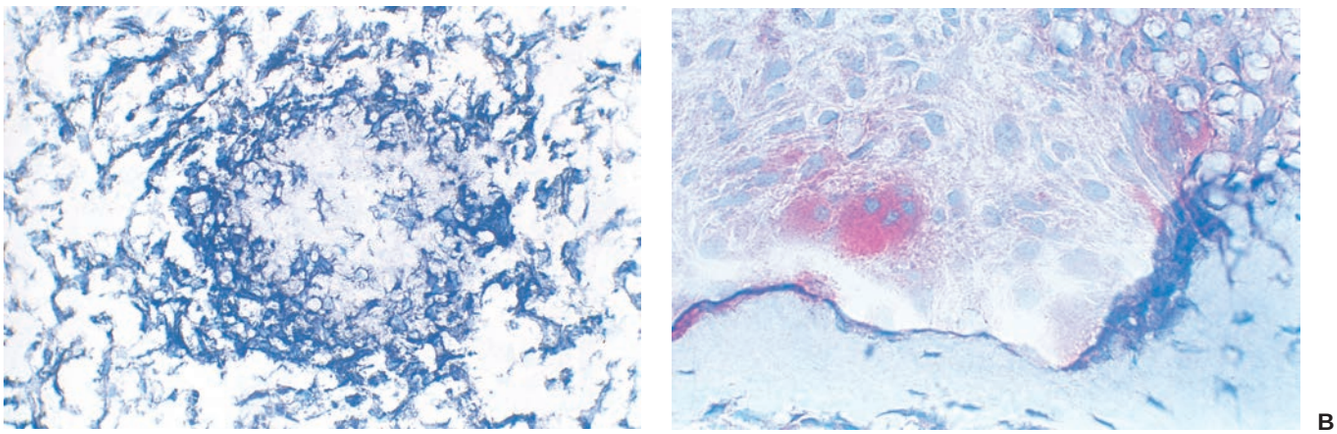

A **B**

Figure 1-37 Enzyme histochemistry. A: Alkaline phosphatase. A small round bone trabecula (*center*) is surrounded by stroma typical for fibrous dysplasia. All cells, in the stroma as well as the osteoblasts at the bone border and osteocytes within the bone, are more or less positive, indicating their bone-forming capability (alkaline phosphatase, original magnification ×50). **B:** Acid phosphatase. In fibrous dysplasia, with reaction for acid phosphatase an osteoclast with four nuclei (*left center*) shows intense activity. The surrounding mononuclear cells show a weak, finely granulated activity. The bone trabecula (*bottom*) shows negative reaction to acid phosphatase marker (acid phosphatase, original magnification ×500).

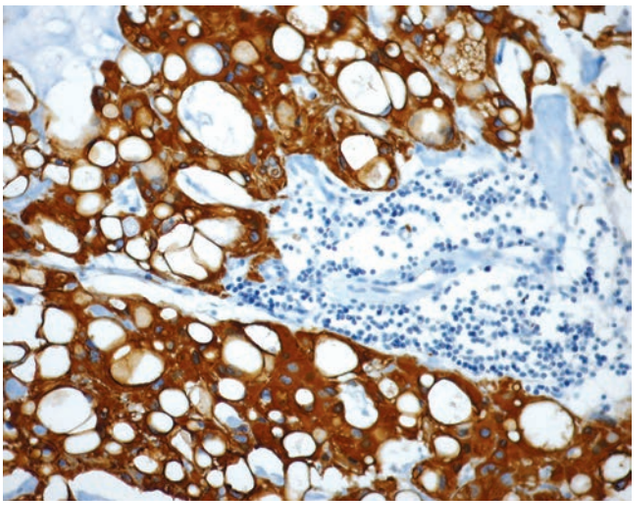

Figure 1-38 Immunohistochemistry. Chordoma. Tumor cells react positive with an antibody-cocktail (CK22) directed against low molecular weight and high molecular weight cytokeratins. Lymphocytes (*center*) and cartilage cells (*upper left*) react negative. Methylene-blue counterstaining (original magnification ×400).

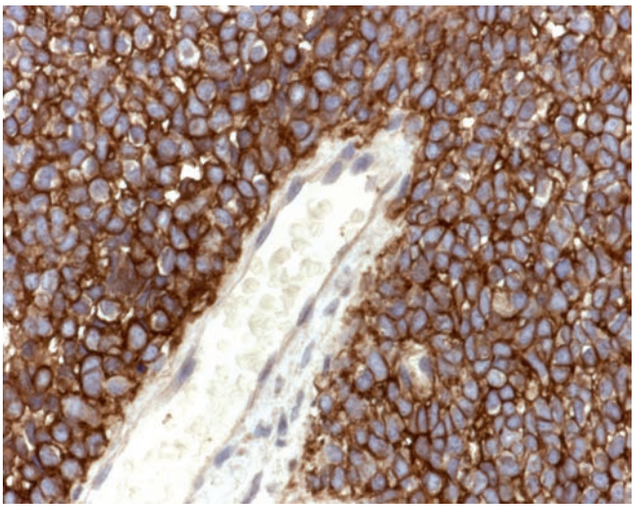

Figure 1-40 Immunohistochemistry. Ewing sarcoma. Tumor cells show a positive membrane-bound reaction for CD99. Nuclei are counterstained with methylene-blue. Centrally located capillary with endothelial cells serve as negative control (original magnification ×400).

hematologic malignancies (82). Most antibodies against these largely cell surface–based antigens have been categorized in workshops and statistically assigned to a so-called cluster of differentiation (CD) number that designates the respective antigen (9,218). These antigens are present not only on lymphatic or hematopoietic (as in Langerhans cell histiocytosis) cells (Fig. 1-39), but also in Ewing sarcoma and synovial sarcoma (CD99) (Fig. 1-40), and in endothelial and vascular tumors (CD31 and CD34). Applied as a panel that must be compiled according to the suspected morphologic differential diagnoses, these antibodies are of great diagnostic help.

Antibodies Against Vascular Antigens

Endothelial cells and endothelial cell–derived tumors are characterized by the expression of Factor VIII–related antigen or von Willebrand factor (Fig. 1-41). This factor is a glycoprotein that is also synthesized in megakaryocytes (170). Because background staining is often seen, especially in hemorrhagic tissue, its use in combination with other endothelial markers, such as

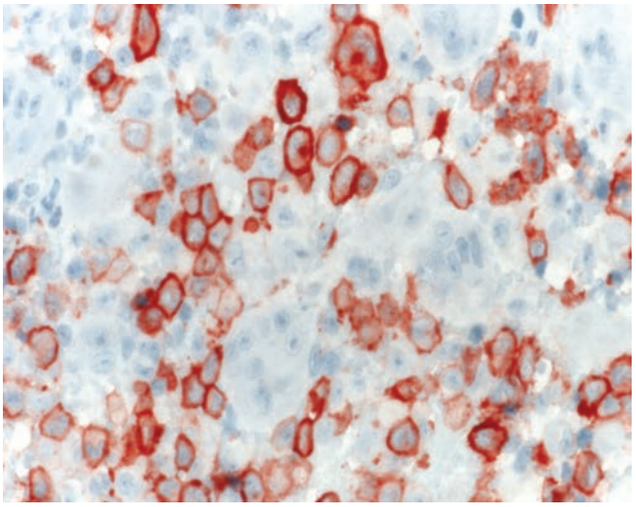

Figure 1-39 Immunohistochemistry. Langerhans cell histiocytosis. Langerhans cells show a strong cytoplasmic immunoreactivity for antibodies against CD1a. Accompanying lymphocytes, macrophages, and giant cells are negative. Methylene-blue counterstaining (original magnification ×400).

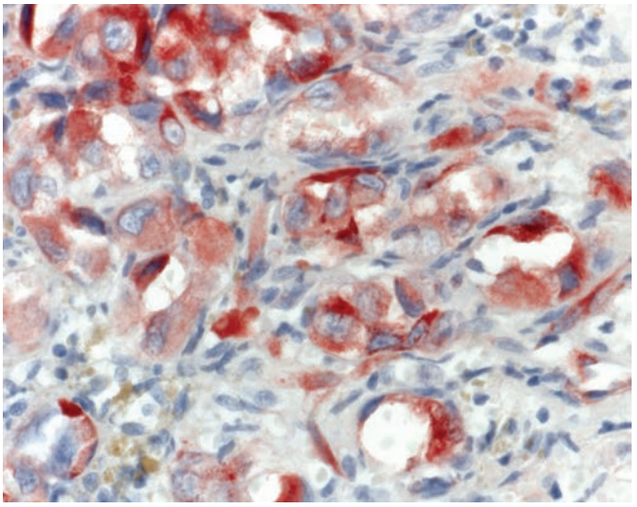

Figure 1-41 Immunohistochemistry. Epithelioid angiosarcoma. Note strong intracytoplasmic immunoreactivity for Factor VIII–related antigen. Methylene-blue counterstaining (original magnification ×400).

CD31 (or platelet-endothelial adhesion molecule) and CD34 (or hematopoietic progenitor cell antigen), is advisable. Both are transmembrane glycoproteins that are expressed in almost all endothelial cells and related tumors (39,124). However, CD34 in particular is also expressed in spindle cell tumors such as hemangiopericytomas, gastrointestinal stromal tumors (GISTs), or solitary fibrous tumors (34).

Antibodies Against Muscle Antigens

For characterization of muscle tissue, antibodies to actins can be used in addition to desmin IHC. Actin is present in all types of cells. By the use of isoelectric focusing, three different groups of actin molecules can be separated—alpha, beta, and gamma actins—consisting of six different isoforms that have been identified by amino acid sequencing as four alpha actins (two sarcomeric—alpha-skeletal and alpha-cardiac muscle actins, and two smooth muscle actins—alpha and gamma, present in the contractile apparatus, and, ultrastructurally, in thin filaments of the respective cells), and two (beta and gamma) nonmuscle cytoskeletal actins (89,204,205). Antibodies to muscle-specific actins are widely used for characterization of muscle tumors (125,166,176,177,184). However, positive immunoreactions have also been observed in osteoblasts, bone marrow stromal cells, osteosarcomas, and malignant fibrous histiocytoma of bone (59,91,202).

Other Useful Antibodies in Bone Tumor Pathology

Enolases are enzymes of the glycolytic pathway. They consist of three different subunits: alpha, beta, and gamma. The functional enzyme is a dimer consisting of two identical subunits (118). The gamma subunit, or neuron-specific enolase (NSE), is found in neural and neuroendocrine cells. Aberrant expression, e.g., in smooth muscle cells, has also been observed (72). NSE positivity is found in PNETs belonging to the Ewing tumor family and in neuroblastomas and melanomas (5,40,147,149).

Synaptophysin is localized in the membrane of presynaptic vesicles. It is a glycosylated acidic protein of 38 KD present in neurons, at neuromuscular junctions, in neuroendocrine cells, and also in PNETs (149,213,214).

In 1965, Moore isolated a protein from bovine brain that was termed S-100 protein because of its solubility in 100% ammonium sulfate. Later it became clear that it comprised a mixture of two structurally related proteins, S-100A and S-100B1 (80,81,131). These belong to an expanding family of small calcium-binding proteins (S-100 protein family) with a molecular weight of 10 to 12 KD, forming homo- and heterodimers (42,119). S-100 proteins are present within cells and nuclei not only in neural tissues but also in Langerhans cells of the epidermis, melanocytes and melanomas, cartilage-derived cells and their tumors, and chordomas (30,137–139,143).

Antibodies to cell cycle–related proteins have recently been applied in bone tumor IHC. Alterations of the cell cycle are considered fundamental to cancer development (88). Particularly in low-grade osteosarcomas and parosteal osteosarcomas, CDK4, a cell-cycle regulator, and MDM2, a regulator of TP53, which normally are not expressed in amounts detectable by IHC, are often overexpressed (159).

The proliferating activity of a tumor can be assessed by identifying all cells that are not in G0-phase of the cell cycle. These cells express a cell stage–related nuclear protein that can be visualized by the MIB1 antibody (90,173).

It should be remembered that IHC is a rapidly expanding field. New markers are described almost every month. They are first considered to be and are announced as "specific" for some tumors. With increasing experience, they become only "characteristic," and are eventually found in a number of different entities. Interpretation of staining results without considering the morphologic context will lead to erroneous assumptions.

Electron Microscopy

At present, the contribution of electron microscopy to the diagnosis of bone tumor is only minimal (Fig. 1-42) (85,203). Ultrastructural investigations can still be of use in the evaluation of small cell neoplasms, spindle-cell tumors, and metastatic disease (111,156). However, these studies are useful only if precise questions, emerging from the evaluation of the routine H&E slides, are addressed, e.g., detection of myofilaments and basal lamina material for discriminating leiomyosarcomas from other spindle-cell sarcomas or Birbeck granules (Fig. 1-43) for identifying a lesion as Langerhans cell histiocytosis (146).

Genetics in Bone Tumors

Genetic investigations have contributed to a better understanding of cancer development. Moreover, some

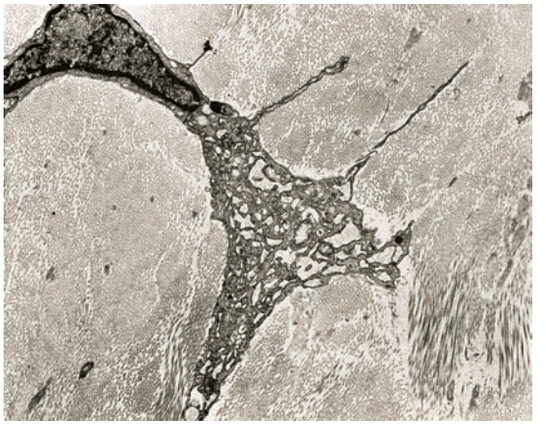

Figure 1-42 Electron microscopy. Fibrous cortical defect. Cell extension (*middle*) containing numerous organelles and the somewhat distorted nucleus (*upper left corner*) is surrounded by stroma with densely arranged immature fibrils. Only a few mature-looking collagen fibrils are seen (*lower right corner*).

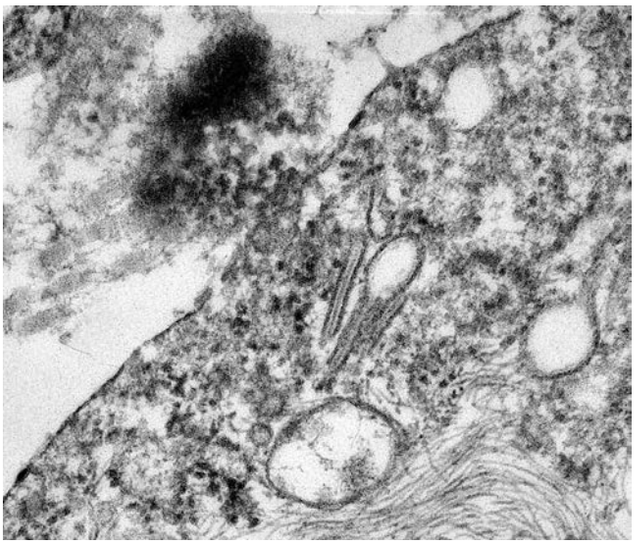

Figure 1-43 Electron microscopy. Langerhans cell histiocytosis. Rod-like and tennis racket–shaped cytoplasmic structures (Birbeck granules; *center*) that present a zipper-like internal core are characteristic for this disorder (original magnification ×64,000).

genetic changes may represent specific cancer signatures such as the translocation of genetic material from chromosome 11 to chromosome 22, which is highly characteristic for Ewing sarcomas. Recent technical advances have dramatically reduced the time interval from the arrival of material at the pathology laboratory to the completion of a genetic analysis as an adjunct to morphologic diagnosis. Some of these methods are briefly discussed in the following sections.

Flow Cytometry

Flow cytometry (FCM) is a quantitative automated method used to analyze the DNA content and the proliferation rate of isolated cells (35,211). To determine the DNA content, the DNA is stained stoichiometrically with specific fluorescent dyes and the emitted fluorescent signal is measured as the nuclei pass one by one through a nozzle-equipped chamber (flow cell). The intensity of the signal is proportional to the amount of DNA in the isolated nuclei. DNA distribution and respective number of cells are calculated, compared with a standard (usually lymphocytes), and then assigned to each phase of the cell cycle (95).

In FCM the total amount of DNA is assessed without considering the distribution of single chromosomes. Therefore, a terminology different from that of cytogenetics has to be applied. The prefix DNA, along with the ploidy terms, is used for FCM investigations. Cells or tumors with the same DNA content as normal control cells, e.g., lymphocytes, are by convention called DNA diploid, whereas cells with less or more DNA are described as DNA aneuploid. Somatic cells ordinarily contain an amount of DNA that is "2C," or diploid, a term reserved for cytogenetic evaluation (77). In the G0 phase, cells are DNA diploid (2C). They then enter the pre-division period, G1 phase, which is followed by the phase of DNA synthesis, the S phase. The number of cells in the S phase of the cell cycle represents the proliferating cell fraction (S-phase fraction, SPF). The amount of DNA gradually doubles until the cells are DNA tetraploid (4C). The cells have reached the premitotic G2 phase, after which mitotic division is performed during the M phase. DNA aneuploid cells contain neither a 2C nor a 4C DNA concentration.

From investigations of epithelial cells and tumors, it is known that DNA aneuploidy and often an increased SPF are found in most carcinomas (50). DNA aneuploidy and increased SPF are also linked to malignancy in cartilaginous tumors (Fig. 1-44). However, studies of endocrine and musculoskeletal tumors have shown that benign aneuploid lesions do exist (3,4). Therefore, the value of FCM as an additional tool for judging proliferating lesions and predicting their biological behavior must be interpreted differently for each tumor type.

Cytogenetics

Cytogenetics is the morphologic study of chromosomes with the use of karyotyping (22). Classical karyotyping still plays a role in the scientific study of many tumors. For identification of numerical and structural aberrations, tumor cells must be freshly obtained, immediately shipped, and cultured in appropriate media. Mitoses of tumor cells can be artificially interrupted during metaphase and the spreaded chromosomes can be stained with special dyes (e.g., Giemsa). This generates a specific transverse pattern ("banding") of each chromosome that can be analyzed. A metaphase chromosome is divided into two arms by a central region, the centromere (the constricted site on the chromosome at which the fibers of the mitotic spindle attach). The short arm is labeled with the letter p, the long arm with the letter q. The chromosomal ends (ter) are called telomeres (tel). The Giemsa-stained, microscopically visible cytogenetic bands or regions can be subdivided at higher magnifications into sub-bands. Both are numbered consecu-

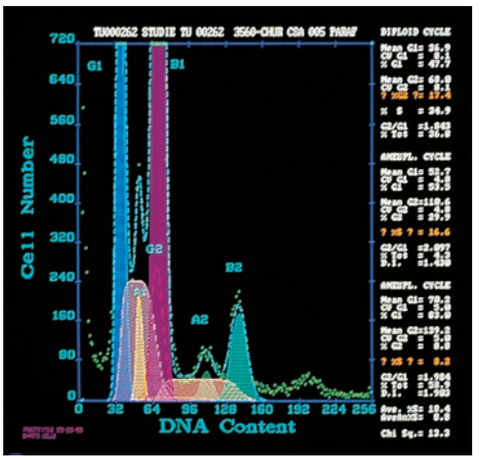

Figure 1-44 Flow cytometry. Chondrosarcoma. Flow cytometry histogram of chondrocytes of grade 2 tumor presents multiploid DNA pattern.